Isogeometric analysis of C^1/G^1 dual mortaring and its application for multi-patch Kirchhoff-Love shell

Di Miao

Advisor: Michael J. Borden

Department of Civil and Environmental Engineering
Brigham Young University
368 CB, Provo, UT 84602, USA

1. Introduction

Isogeometric analysis was introduced by Hughes et. al. [49] in 2005, as a novel discretization technology. Since then, it attracted considerable attentions from the acedamic world and is enjoying explosive growth. The idea behind isogeometric analysis is to use the same basis functions for the geometric modeling and computational analysis. While the main aim of isogeometric analysis is to eliminate the geometric approximation error, it has been observed that, compared to traditional C^0 finite element, higher regularity Non-uniform Rational B-splines (NURBS) provide higher efficiency per degree of freedom [5, 29, 30]. Meanwhile, high regularity basis functions allow us to solve higher order partial differential equations (PDEs), e.g. the biharmonic equation [66, 56, 53], the Kirchhoff-Love shell problem [58, 57, 59] and the Cahn-Hilliard equation [42, 17, 16].

However, the higher dimensional NURBS basis functions are obtained by a tensor product of one-dimensional NURBS basis functions, which imposes limitations on its feasibility for analysis. Considering a scenario that a refinement is applied to a region of interest, however, for the tensor-product domain, it also introduces control points far from that region, which dramatically increases the problem size.

The adaptive finite element technique try to automatically refine a mesh in an optimal fashion so that a desirable discretization error level is achieved

with the fewest degrees of freedom. Based on the solution from a coarse mesh, a *posteriori* error estimator provides a guidance for deciding where and how to refine a mesh. It can increase the convergence rate, particularly when singularities are present. However, this promising technique can not be applied directly to NURBS mesh, as it does not support local refinement.

Since high smoothness basis function can be used in Isogeometric analysis, the numerical approximation of high order PDEs can be realized in the framework of the standard Galerkin formulation. However, without introducing mesh degenerations, it is impossible to parameterize geometries with sharp corner or kink by high continuity meshes.

2. Literature review

To circumvent the shortcomings discussed above, various methods have been proposed. The purpose of this section is to provide an overview of the popular methods that endow B-spline meshes with multi-patch coupling and local refinement abilities.

2.1. Local refinable splines

In 1988, Forsey and Bartels [40] introduced the hierarchical B-spline refinement algorithm, which can restrict the influence of refinement to the locality. The algorithm is achieved by a re-representation process that replaces each basis function by an equivalent linear combination of a set of basis functions defined by nested knot vectors. However, due to the lack of a natural control grid, the hierarchical B-spline has not been widely recognized in the CAD society, and a few applications can be found in geometric design. Recently, this technique has been extended to Isogeometric Analysis, by Vuong *et al.* [86]. Owing to the construction strategy, the resulted hierarchical basis function are linearly independent and retain the maximal regularity, which renders the hierarchical B-spline a good candidate for analysis. The numerical tests demonstrate that the use of the hierarchical B-spline lead to a superior performance for problems with corner singularity. A subdivision-based hierarchical B-spline was proposed by Bornemann *et al.* [18], to tackle the intricate algorithms in the software implementation of hierarchical B-splines. The subdivision scheme establishes algebraic relations between the basis functions and their coefficients defined on different refinement level of the mesh and greatly ease the implementation of hierarchical B-splines. Consecutively, the truncated basis for hierarchical splines (THB-spline) was

introduced by Giannelli *et al.* [41]. THB-splines is created by eliminating from the coarse hierarchical basis function the contribution corresponding to the subset of finer basis functions. Besides all the nice properties of hierarchical B-splines, the THB-splines obtain smaller support and form a partition of unity, which lead to sparser matrices and lower condition numbers.

However, all the above hierarchical B-splines are still under the tensor product formulism, which restricts hierarchical B-splines to a global rectangular parametric domain. In order to represent complex topologies, subdivision schemes are widespread in geometry processing and computer graphics. Among the most popular subdivision schems are the Catmull-Clark [23], Doo-Sabin [31] and Loop's [64] scheme. For Isogeometric Analysis, Wei *et al.* [87] introduced truncated hierarchical Catmull-Clark subdivion (THCCS) that can handle extraordinary nodes involved in complex topologies. THCCS inherits the surface continuity of Catmull-Clark subdivision, namely C^1 continuity at extraordinary points and C^2 continuity elsewhere. Loop subdivision surfaces provides similar regularity properties as THCCS and has been applied to Isogeometric Analysis in [52, 70] to generate triangular meshes. One of the limitations in the implementation of subdivision meshes is that the basis function around the extraordinary point is composed of piecewise polynomial functions with an infinite number of segments, which leads to insufficient integration by Gauss quadrature rule. To deal with this issue, various quadrature rules and adaptive strategies have been examined in [67] for Poisson problem on the disk and in [51] for fourth order PDEs.

In 2003, Sederberg *et al.* [78] introduced T-splines, which allows the existence of T-junctions in the control grid, so that lines of control points need not traverse the entire control grid. Thus, local refinement can be realized by introducing T-junctions around interested region. Since the concept of T-splines is a generalization of NURBS technology, it can be used to merge NURBS surfaces that have different knot-vectors at the intersection. Therefore, the T-splines are also suitable to address trimmed multi-patch geometries. Due to the desirable features of T-splines, Bazilevs *et al.* [4] explored this technology in Isogeometric Analysis, and numerical results demonstrated its potential for solving structural and fluid problems. By utilizing the Bézier extraction operator, a finite element data structure for T-splines [77] was developed to ease the incorporation of T-splines into existing finite element codes. However, it has been proven [22] that the original definition of T-splines is not sufficient to ensure the linear independence of the basis functions. To circumvent this issue, analysis suitable T-splines [63]

3

was developed by applying an additional constraint that no two orthogonal T-junction extensions are allowed to intersect. Subsequently, the mathematical properties of analysis suitable T-splines were studied in [62, 90], and it has been sucessfully applied to the boundary element method [76]. Meanwhile, an adaptive local h-refinement algorithm with T-splines and a local refinement of analysis-suitable T-splines were introduced by Döfel *et al.* [37] and Scott *et al.* [75], respectively. However, for both algorithm, the refined mesh is not as local as one could hope and this problem might be severe in 3D.

2.2. Multi-patch geometrically continuous functions

One of the advantages of Isogeometric Analysis is that it provides basis functions with high smoothness, *i.e.* for p-th order splines, they enjoy up to C^{p-1} continuity within a single patch. Thus, it is possible to directly discretize differential operators of order higher than 2. However, continuity higher than C^0 for multi-patch discretization imposes significant difficulties. The conception of geometric continuity is very important in CAD field [72] for designing smooth multi-patch domain containing extraordinary vertices [71]. In the parametric space, the geometric continuity of order s (G^s continuity) is a weaker continuity constraint as compared to C^s continuity, while it has been proved by Groisser and Peters [43] that G^s continuity in the parametric space is equivalent to C^s continuity of the basis function after the parametric mapping. Thus, the construction of C^s isogeometric functions over a C^0 parameterization can be interpreted as geometric continuity G^s of the graph parameterization. Bercovier *et al.* [12] has shown that for multi Bézier patches over an unstructured quadrilateral mesh, as long as the order of polynomial is high enough, there always exists the minimal determining set for a C^1 continuity construction. Moreover, the resulting basis functions do not contain subdivisions around extraordinary vetices.

The case of G^1 continuous functions on bilinearly parametrized two-patch B-spline domains was considered by Kapl *et al.* [56], where the C^1 basis functions are constructed and analyzed by numerical tests. It is shown that the space dimensionality heavily depends on the parameterization of two bilinear patch, and optimal convergence is observed on biharmonic problem. However, over-constrained C^1 isogeometric spaces that causes sub-optimal convergence is also observed for certain configurations (*e.g.* two-patch non-bilinear parameterizations and C^{p-1} continuity within the patches for p-th order spline space). A theoretical analysis of the causing of C^1 locking is

4

provided in [25], where the analysis-suitable G^1 geometry parameterization, that allows for optimal approximation of C^1 isogeometric spaces, is identified and testified by numerical examples. The methods in [56] has been extended to bilinearly parameterized multi-patch domains in [53], where the simple explicit formulas for spline coefficients of C^1 basis function is derived and nested C^1 isogeometric spaces are generated. Recently, Kapl *et al.* [55, 54] explored the construction of C^2 isogeometric functions on multi-patch geometries and utilized the C^2 isogeometric spaces for 6-th order PDE.

Although the geometrically continuous functions circumvent the use of subdivisions for domains with extraordinary vertices, the requirement of C^0 parameterization averts local mesh refinement, and lower continuity is required to avoid C^1 locking effect. Thus, its implementation can be complex and it may not be a potential candidate for analysis in more general situations.

2.3. Variational approach for domain coupling

Unlike geometric design, where high continuity basis functions along the intersections of neighboring patches are required for the construction of high quality surface; in analysis, these strong point-wise constraints are unnecessarily rigorous, a good approximation of PDEs can be made even if these constraints are applied in the weak sense. Moreover, the non-conforming multi-patch coupling is allowed, which maintains the flexibility for the choice of meshes when multi-patch discretization is needed. Mathematically, the error estimation of the non-conforming finite element approximation is based on Strang's lemma [20, 82], which says that for the non-conforming discretized PDEs, the distance between exact solution to the discrete one is bounded by the sum of the approximation error and the consistency error. The approximation error measures the failure of discretized finite dimensional space to capture the exact solution, while the consistency error measures the inconsistency between the exact equation and the discretized equation. Various methods have been developed to eliminate the consistency error and recover optimal convergence, among them are the mortar method (Lagrange multiplier method), stablized Lagrange multiplier method, the Nitsche's method and the discontinuous Galerkin (dG) method.

To clearly demonstrate these methods, we consider the following Poisson

problem with homogenesous Dirichlet boundary conditions

$$
\begin{aligned}
-\Delta u &= f, && \text{in } \Omega \\
u &= 0, && \text{on } \partial\Omega
\end{aligned}
\tag{1}
$$

where Ω denote a bounded open domain in $\mathbb{R}^d$, $d = 2$ or 3 being the dimension of the problem and its boundary is denoted by $\partial\Omega$, in order to simplify the presentation we restrict ourselves to the case of two-dimensional computational domain. The weak form of Equation (1) reads as follow: Find $u \in H_0^1(\Omega)$ such that

$$
a(u, v) = l(v), \qquad \forall v \in H_0^1(\Omega),
\tag{2}
$$

where

$$
\begin{aligned}
a(u, v) &= \int_\Omega \nabla u \cdot \nabla v\, d\Omega, \\
l(v) &= \int_\Omega f v\, d\Omega.
\end{aligned}
\tag{3}
$$

Using the fact that $C^0(\Omega) \subset H^1(\Omega)$, the weak solution can be approximated by considering a finite dimensional continuous function space. Now, we assume that the domain Ω is subdivided into K non-overlapping subdomains or patches Ω_k for $1 \le k \le K$, i.e.

$$
\bar{\Omega} = \bigcup_{k=1}^{K} \bar{\Omega}_k \quad \text{and} \quad \Omega_k \bigcap \Omega_l = \emptyset \quad \forall k \ne l.
\tag{4}
$$

For simplicity, we only consider the case that the intersection of two patches is either empty or vertex or the entire edge, which rules out the possibility of hanging nodes. We denote the common interface of two neighboring subdomains $\Gamma_{kl} = \partial\Omega_k \bigcap \partial\Omega_l$ so that $\Gamma_{kl} = \emptyset$ if Ω_k is not a neighbor of Ω_l and define the skeleton $\mathbf{S} = \bigcup_{k,l \in K, k \ne l} \Gamma_{kl}$ as the union of all interfaces. A representative example of geometry is presented in Figure 1. We can associate each subdomain a bijective geometric mapping as

$$
\mathbf{F}_k\left(\xi_k, \eta_k\right) : \hat{\Omega}_k \mapsto \Omega_k \in \mathbb{R}^d,
\tag{5}
$$

where $\hat{\Omega}_k$ is the parametric domain of kth patch associated with coordinates (ξ_k, η_k). For the simplicity and without loss of generality, we assume
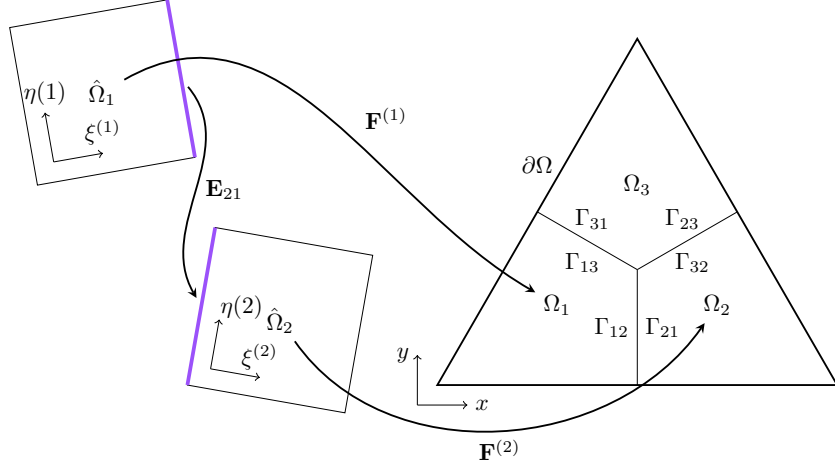
Figure 1: An example of domain decomposition, patches are defined on different parametric domains and are connected via geometric mapping.

$\hat{\Omega}_k = [0,1] \times [0,1]$ for all patches. Due to the difference in the patch parameterizations, a physical point on the interface can be mapped to different parametric domains with different coordinates. Owing to non-singular parameterization, we can establish a bijective transformation from the shared edge of $\hat{\Omega}_k$ to that of $\hat{\Omega}_l$ by

$$\mathbf{E}_{kl} = (\mathbf{F}_l)^{-1} \circ \mathbf{F}_k. \tag{6}$$

For each Ω_k, we introduce the function space

$$H^1_*(\Omega_k) := \left\{ u \in H^1(\Omega_k) : u = 0 \quad \text{on } \partial\Omega \bigcap \partial\Omega_k \right\}, \tag{7}$$

now we can define the broken Sobolev space

$$\mathcal{X} := \left\{ u \in L^2(\Omega) : u|_{\Omega_k} \in H^1_*(\Omega_k) \right\}. \tag{8}$$

Now, the question is how to approximate the weak solution of Equation (2) from a finite dimensional subspace of $\mathcal{X}$. Since functions in $\mathcal{X}$ can be discontinuous on the skeleton $\mathbf{S}$, $a(u,u)$ is no longer coercive (or V-elliptic) on $\mathcal{X}$. As a result, directly using a finite dimensional subspace of $\mathcal{X}$ to discretize Equation (2) will lead to a non-invertible stiffness matrix. Modifications to the weak form is needed, and we will review some of the most popular methods in this section.

2.3.1. Lagrange multiplier method

The Lagrange multiplier method (or sometimes called mortar method)
is a domain decomposition technique that allows the coupling of different
discretization schemes or of non-matching triangulation along interior inter-
faces. The inter-element continuity condition is enforced weakly by Lagrange
multipliers. For the Poisson problem, the C^0 continuity constraint is required
on the intersections, in other words, the jump on the skeleton

$$[u]_{\Gamma_{kl}} := u_k - u_l = 0, \quad \forall \quad \Gamma_{kl} \in \mathbf{S}, \tag{9}$$

where $u_k = u|_{\Omega_k}$. In order to apply the constraint to the weak form, we
introduce the potential energy functional:

$$\Pi(v) := \frac{1}{2}a(v,v) - l(v). \tag{10}$$

The Equation (2) is equivalent to the minimization problem:

$$\inf_{v \in H_0^1(\Omega)} \Pi(v). \tag{11}$$

Then, given a function space $\mathcal{M}$ defined on the skeleton, a Lagrange multi-
plier $\mu \in \mathcal{M}$ is used to add the constraint (9) to the potential energy func-
tional (10), and the resulted the potential energy functional for the Lagrange
multiplier method reads

$$\Pi_{LM}(v,\mu) := \Pi(v) + b(\mu,v), \tag{12}$$

where

$$b(\mu,v) = \sum_{\Gamma \in \mathbf{S}} \int_\Gamma \mu\, [u]_\Gamma\, d\Gamma. \tag{13}$$

The variational formulation of the Lagrange multiplier problem can be de-
rived from the saddle point problem of the potential energy functional (12)

$$\inf_{v \in X} \sup_{\mu \in \mathcal{M}} \Pi_{LM}(v,\mu), \tag{14}$$

as, find $(u,\lambda) \in \mathcal{X} \times \mathcal{M}$ such that

$$\begin{cases} a(u,v) + b(v,\lambda) = l(v) & \forall v \in \mathcal{X}, \\ b(u,\mu) = 0 & \forall \mu \in \mathcal{M}. \end{cases} \tag{15}$$

The solution of the variational formulation is the infimum in v and the supremum in μ, in other words, it is still a minimization problem in terms of the primary varible v and any function that violate the constraint will be eliminated by the Lagrange multiplier μ. This is the reason why it is called the saddle point problem. We also denote that the physical meaning of the Lagrange multiplier μ for (12) is the flux of v over the skeleton. A comprehensive study of the mixed problem (15) can be found in [15].

In the discretized problem, for a given discrete space $\mathcal{X}_h$, the choice of the discrete Lagrange multiplier space $\mathcal{M}_h$ plays a fundamental role for the stability of the saddle point problem and the optimality of the discretization scheme. To ensure the optimality, the function space for Lagrange multiplier should be judiciously chosen so that the consistency error should converges at the same rate as that of the approximation error. The feasibility of the discrete space pair $\mathcal{X}_h \times \mathcal{M}_h$ can be measured by the inf-sup test. The inf-sup condition is also refered to as the Ladyzhenskaya-Babuska-Brezzi condition (or simply LBB). It is a crucial condition to ensure the solvability, stability and optimality of a mixed problem. For the problem (15), the inf-sup condition is [15], for $v \neq 0$ and $\mu \neq 0$

$$\inf_{\mu \in \mathcal{M}} \sup_{v \in \mathcal{X}} \frac{|b(v, \mu)|}{\|v\|_{\mathcal{X}} \|\mu\|_{\mathcal{M}}} \geq \beta > 0. \tag{16}$$

Since the approximation error of problem (15) is given as

$$\|u - u^h\|_{\mathcal{X}} + \|\lambda - \lambda^h\|_{\mathcal{M}} \leq C \left(\inf_{u^h \in \mathcal{X}^h} \|u - u^h\|_{\mathcal{X}} + \inf_{\lambda^h \in \mathcal{M}^h} \|\lambda - \lambda^h\|_{\mathcal{M}} \right), \tag{17}$$

where C is a constant that depends on variables including β but is independent of the mesh size h. Hence, in a discretized problem, the inf-sup condition requires the variable β to be a constant that is independent of the mesh size.

It is well-known that in order to satisfy the LBB-condition a number of possible natural choices for the approximation space pair $\mathcal{X}_h \times \mathcal{M}_h$ must be discarded. In particular, the trace space of slave side, specially convenient from the computational point of view, often do not satisfy the LBB-condition and can activate pathologies such as spurious oscillations. To remedy this problem, the most widely used method in the finite element framework is reducing the dimension of Lagrange multiplier space by two (for 2nd order PDEs). Specifically, the degree of Lagrange multiplier basis functions at both
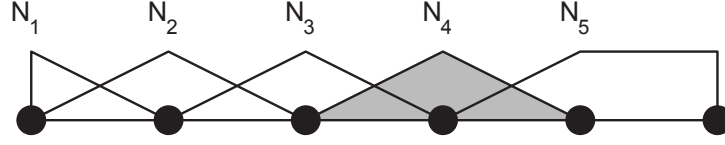
9

Figure 2: Lagrange multiplier basis functions for the piecewise linear elements, modification on the right end (from Zienkiewicz [91]).

ends are reduced by one. This modification has been successfully adopted in [14, 13, 7, 10, 8, 65, 60, 9]. An example of the modified Lagrange multiplier basis functions are illustrated in Figure 2, where the basis function N_5 is constant in the right end.

In the context of Isogeometric Analysis, the patch coupling problem has been firstly studied by Hesch and Betsch [47], where the coupling of Lagrangian elements and NURBS elements for 3D nonlinear elastic problem is validated. To avoid an over constrained linear system, Hesch and Betsch used a linear Lagrange multiplier space for higher order NURBS coupling. In [21], the choice of the Lagrange multiplier space has been extensively studied, it testifies that for equal order pairing, a local degree reduction at extraordinary vertices is required, and another possibility is reducing the degree of Lagrange multiplier space by two compared to the trace space of slave side. These choices of Lagrange multiplier spaces are proven to be inf-sup stable by various numerical examples. In addition to the constraint on the interpatch displacement, Bouclier *et al.* [19] considered the constraint on the traction and claimed that this strategy enables to present a C^1 behavior. In the numerical test, smoother displacement fields and smoother stress fields are observed.

Another drawback of the implementation of mortar methods is that most of them introduce Lagrange multipliers as additional variables to enforce interface constraints weakly, increasing the problem size. Moreover, different physical fields are involved in the weak form, deteriorating the conditioning of the global matrix if no appropriate pre-conditioner is applied (detailed discussion about preconditioning for saddle point problem can be found in [39, 11, 83]).

10

273 *2.3.2. Dual mortar method*

274   To circumvent the increase of problem size, we considering the minimiza-
275 tion problem

$$\inf_{v \in \mathcal{K}} \Pi(v), \tag{18}$$

276 where the function space $\mathcal{K} = \{v \in \mathcal{X} : b(v, \lambda) = 0, \forall \lambda \in \mathcal{M}\}$. The mini-
277 mization problem (18) is indeed equivalent to the saddle point problem (15),
278 the proof can be found in [15]. Note that, since $K \subset X$, the introduce of
279 Lagrange multiplier indeedly reduces the problem size of (18). Meanwhile,
280 the symmetric positive definite structure of the resulting stiffness matrix is
281 preserved. But the construction of the function space K is not a trivial task.
282   To reduce the cost of constructing the function space $\mathcal{K}$, we use the dual
283 basis functions of the trace space of the slave side as the discrete Lagrange
284 multiplier space. For a given basis function N_i, the dual basis function $\hat{N}_j$ is
285 defined to satisfy

$$\int_\Gamma N_i \hat{N}_j d\Gamma = \delta_{ij} \int_\Gamma N_i d\Gamma, \tag{19}$$

286 where δ_{ij} is a Kronecker delta function. Of special interest, are biorthogonal
287 basis functions with compact support, especially

$$\operatorname{supp} \hat{N}_i = \operatorname{supp} N_i. \tag{20}$$

288 Due to the biorthogonality, the discrete bilinear form $b(v, \mu)$ forms a diagonal
289 matrix on the slave side, and forms a sparse matrix on the master side.
290 The function space $\mathcal{K}$ can be formulated without additional efforts and all
291 the slave degree of freedom are eliminated in the resulting linear system.
292 Moreover, owing to the local support property the resulting stiffness matrix
293 is a symmetric positive definite sparse matrix. Thus, the dual basis functions
294 are very attractive in the perspective of computational efficiency.
295   Figure 3 shows an example of dual basis functions corresponding to the
296 basis functions in Figure 2. Again, order reduction is made at the right end.
297 The dual mortar method was first introduced in [88] for first order finite
298 element. This method has been extended to higher order degree elements in
299 [61], to three-dimensional problem in [89] and to contact problem [48, 73].
300   In isogeometric analysis framework, a master-slave type mortar method
301 has been suggested by Dornisch *et al.* [34], where the weakly applied con-
302 straint is represented as a master-slave relation and the the slave interface
303 degrees of freedom (DOF) can be condensed out of the global linear system.
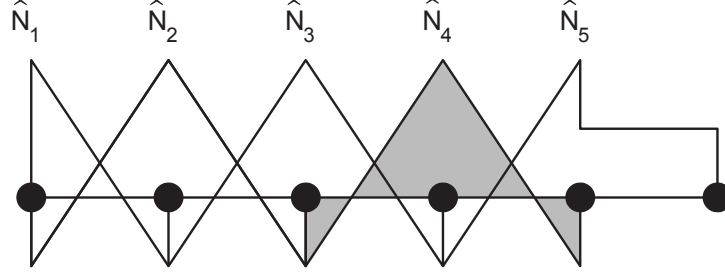
11

Figure 3: Dual Lagrange multiplier basis functions for the piecewise linear elements, modification on the right end (from Zienkiewicz [91]).

Recently, Dornisch *et al.* extended this research to multiple patch coupling in [36, 33], where different types of dual basis functions are applied as the basis of Lagrange multipliers. The numerical results demonstrate that the approximate dual basis functions yield accurate result and generate sparse global matrix due to the local support. The concept of dual mortar methods is also utilized in [79] for contact problem in Isogeometric analysis framework. Coox *et al.* [27] proposed an interesting approach to establish the master-slave mortar method and implemented this approach in [26] to form boundary element analysis on complex manifold. In this approach, the master-slave relation are formed by knot insertion algorithm and pseudo-inverse.

2.3.3. Perturbed Lagrangian method

Applying constraint by Lagrange multiplier leads to a saddle point problem, of which the discrete Lagrange multiplier basis functions cannot be chosen independently of that of primal variable and special treatment is required on the cross point to ensure the solvability and optimality of the discretized system. The stiffness matrix for the discrete problem arising from the Lagrangian multiplier method always contains both positive and negative eigenvalues, for which iterative methods are known to be less efficient than for symmetric positive definite systems. To ensure the invertibility of the stiffness matrix, a quadratic penalty term is added to the energy functional (12), as

$$\Pi_{PLM}(v, \mu) := \Pi_{LM}(v, \mu) - \frac{1}{2\epsilon} \sum_{\Gamma \in \mathbf{S}} \int_{\Gamma} \mu^2 d\Gamma, \tag{21}$$

where the penalty term is scaled by a parameter ϵ. The resulted functional (21) is refered to as perturbed Lagrangian and the last term is often

called stablization term. The resulted variational formulation is stated as

$$
\begin{cases}
a(u,v) + b(v,\lambda) = l(v) & \forall v \in \mathcal{X}, \\
b(u,\mu) - \frac{1}{\epsilon} \sum_{\Gamma \in \mathbf{S}} \int_{\Gamma} \mu\lambda d\Gamma = 0 & \forall \mu \in \mathcal{M}.
\end{cases}
\tag{22}
$$

As $\epsilon \to \infty$, the solution obtained from (22) will converge to the solution obtained by the classical Lagrange multiplier method. For $0 < \epsilon < \infty$, any solution that inconsistent with the constraint will not be fully prohibited, but will be penalized by the stability term. And the rank of discrete stiffness matrix is preserved no matter whether the discrete space pair $\mathcal{X}_h \times \mathcal{M}_h$ fulfills the inf-sup condition or not. However, for a moderate ϵ, the perturbed Lagrangian method is inconsistent with the classical Lagrange multiplier method, and the increase of ϵ will deteriorate the conditioning of stiffness matrix.

The perturbed Lagrangian method has been utilized in [80] for contact problem and [35, 1] for domain decomposition problem in isogeometric analysis framework.

2.3.4. Stablized Lagrange multiplier method

To fully circumvent the inf-sup condition for imposing Dirichlet boundary by Lagrange multiplier, Barbosa et. al. [3] added a new penalty like term to the energy functional (12) to enhance the stability. Unlike perturbed Lagrangian method where the penalty term is inconsistent with the original problem, the new term proposed by Barbosa maintaining the consistency. The energy functional of stablized Lagrange multiplier method is given as

$$
\Pi_{SLM}(v,\mu) := \Pi_{LM}(v,\mu) - \sum_{\Gamma \in \mathbf{S}} \frac{h}{2\gamma} \int_{\Gamma} (\mu + \left\{ \frac{\partial v}{\partial n} \right\})^2 d\Gamma,
\tag{23}
$$

where n is the normal vector of the interface, h is the mesh size on the intersection, γ is a user defined constant, the average operator

$$
\{u\}_{\Gamma_{kl}} := \frac{1}{2} u_k + \frac{1}{2} u_l.
\tag{24}
$$

Since the physical meaning of the Lagrange multiplier is the flux on the intersection, the stabilization term in (23) is consistent with the original problem. The resulted variational formulation is stated as

$$
\begin{cases}
a(u,v) + b(v,\lambda) - \frac{h}{\gamma} \sum_{\Gamma \in \mathbf{S}} \int_{\Gamma} \frac{\partial v}{\partial n}(\lambda + \left\{\frac{\partial u}{\partial n}\right\}) d\Gamma = l(v) & \forall v \in \mathcal{X}, \\
b(u,\mu) - \frac{h}{\gamma} \sum_{\Gamma \in \mathbf{S}} \int_{\Gamma} \mu(\lambda + \left\{\frac{\partial u}{\partial n}\right\}) d\Gamma = 0 & \forall \mu \in \mathcal{M}.
\end{cases}
\tag{25}
$$

13

The stabilization parameter γ needs to be carefully chosen. If γ is too large, the method degrades to a penalty-type method, with sub-optimal accuracy in the asymptotic limit. If γ is too small, the method becomes unstable. Recall the trace inequality

$$\|h^{\frac{1}{2}}\frac{\partial u}{\partial n}\|^2_{\partial\Omega_k} \leq C\|\nabla u\|^2_{\Omega_k}. \tag{26}$$

It has been shown [50] that the mixed formulation (25) fulfills the inf-sup condition if $\gamma > 2C$. The constant C can be approximated by discretize the norms in the inequality (26) and solve the resulting discrete eigenvalue problem.

It has been demonstrated that there is a close connection with the stablized Lagrange multiplier method and Nitsche's method in the context of setting the Dirichlet boundary conditions [81] and in the context of domain decomposition [46, 45, 50]. Tur et. al. [85] utilized this method to solve both small and large deformation contact problems and obtained optimal convergence rate for linear elements. To our knowledge, this method has not been applied in the isogeometric analysis framework yet.

2.3.5. Discontinuous Galerkin method

Discontinuous Galerkin method (or Nitsche's method) was introduced in 1971 [69] for handling Dirichlet boundary conditions in the weak sense. Discontinuous Galerkin method resembles a mesh-dependent penalty method. Unlike the standard penalty method, which is not consistent unless the penalty coefficient goes to infinity, discontinuous Galerkin method is consistent with the original problem. Moreover, no additional unknown (Lagrange multiplier) is needed and no discrete inf-sup condition must be fulfilled, contrarily to mixed methods. Meanwhile, additional term are added into the weak form to ensure the ellipticity of the problem.

To develop the weak form of discontinuous Galerkin method for homogeneous Poisson problem, we start by multiplying (1) by a test function $v \in X$ and integrating by parts, we obtain

$$a(u,v) - \sum_{\Gamma\in\mathbf{S}}\int_\Gamma \left\{\frac{\partial u}{\partial n}\right\}[v]\,d\Gamma = l(v). \tag{27}$$

However, if we consider the right-hand side as a bilinear form, it is not coercive. In other words, this problem is not well-posed, since coercive implies

14

the uniqueness of solution. Meanwhile, this bilinear form is not symmetric. To recover the symmetry and coercivity of the bilinear form, additional terms are needed. To maintain the consistency, the added terms must vanish for the true solution. This lead to the following weak form: find $u \in X$ such that

$$a(u,v) - \sum_{\Gamma \in \mathbf{S}} \int_\Gamma \left\{ \frac{\partial u}{\partial n} \right\} [v] \, d\Gamma - \epsilon \sum_{\Gamma \in \mathbf{S}} \int_\Gamma \left\{ \frac{\partial v}{\partial n} \right\} [u] \, d\Gamma + \sum_{\Gamma \in \mathbf{S}} \frac{\gamma}{h} \int_\Gamma [u] \, [v] \, d\Gamma = l(v) \quad \forall v \in \mathcal{X}. \tag{28}$$

Since $[u] = 0$ on the intersections, the above formulation is consistent with (27). Furthermore, and as already stated in [74] the parameter ϵ can be set to some particular values, namely:

- For $\epsilon = +1$, the resulting method is called the symmetric interior penalty Galerkin (SIPG) method. The stiffness matrix of SIPG is symmetric.

- If $\epsilon = 0$, we obtain the incomplete interior penalty Galerkin (IIPG) method. It involves only a few terms and is of easiest implementation.

- If $\epsilon = -1$, the resulting method is called the nonsymmetric interior penalty Galerkin (NIPG) method. It admits one unique solution and converges optimally irrespectively of the value of $\gamma > 0$.

For $\epsilon = 0$ and $\epsilon = +1$, the bilinear form is coercive if $\gamma > C$ and $\gamma > 2C$, respectively [74]. Similar to the stablized Lagrange multiplier method, the discontinuous Galerkin method also requires to solve an eigenvalue problem to determine the value of γ.

Discontinuous Galerkin method has been widely studied in various aspects, including imposing boundary condition [45], domain decomposition [6] and contact problem [24]. In the field of Isogeometric analysis, Discontinuous Galerkin method has been utilized to imposing Dirichlet boundary condition for trimmed spline meshes [38]. The first article discussing discontinuous Galerkin method based domain decomposition strategy was written by Apostolatos *et al.* [2]. Nguyen *et al.* extended it to three-dimensional problems in [68]. Guo *et al.* [44] proposed a Nitsche's method for coupling Kirchhoff-Love NURBS shell patches. Since the governing equation for

15

Table 1: Property comparison of Lagrange multiplier, dual mortal, perturbed Lagrange multiplier, stablized Lagrange multiplier and discontinuous Galerkin methods.

Methods	well-defined	inf-sup	symmetry	positive definite	size
Lagrange multiplier	depends	depends	yes	no	enlarged
Dual mortar	yes	depends	yes	yes	reduced
Perturbed Lagrange multiplier	yes	depends	yes	no	enlarged
Stablized Lagrange multiplier	depends	yes	yes	no	enlarged
Discontinuous Galerkin	depends	yes	depends	yes	same

Table 1: Property comparison of Lagrange multiplier, dual mortal, perturbed Lagrange multiplier, stablized Lagrange multiplier and discontinuous Galerkin methods .

Kirchhoff-Love shell is 4-th order PDE, C^1 continuity constraint in imposed weakly in the method.

Although discontinuous Galerkin method does not introduce additional DOF and does not need the judicious choice of mutiplier function space, the value of the constants in the stablizing term need to be determined. Normally, they are determined by solving a eigenvalue problem on the domain of the combination of all intersections, which leads to extra computational cost. Meanwhile, the additional stablizing terms reduce the sparsity of the global linear system. For higher order PDEs, discontinuous Galerkin method becomes more complex as higher order derivatives exists in the tractions.

A comparison of the variational coupling methods discussed above is shown in Table. 1.

3. Research Objectives

My dissertation research focuses on the construction of NURBS basis functions among multi-patches that are analysis-suitable for 4th order PDEs. The coupling constraints are applied weakly by using the dual mortar method. The dual basis functions are constructed based on the Bézier probjection technology proposed in [84].

4. Preliminaries

This section provides the formulation of univariate basis functions, its extention to higher dimensional space, and representations of geometries in the context of Isogeometric Analysis. For a detailed explanation we refer to.

4.1. Univariate B-spline basis functions

A univariate B-spline is peicewise polynomial curve represented as a linear combination of B-spline basis functions. Basis functions of pth order B-spline with n degrees of freedom can be defined by a non-decreasing set of real numbers

$$\Xi = \{\xi_1, \xi_2, \cdots, \xi_{n+p+1}\}, \tag{29}$$

which is called knot vector. B-splines that are interpolatory at the ends can be achieved by requiring the multiplicity of $p+1$ for the first and the last knot. Associated B-spline basis functions are defined using the Cox-de Boor recursion formula:

$$N_{i,0}(\xi) = \begin{cases} 1 & \xi_i \leq \xi \leq \xi_{i+1} \\ 0 & otherwise \end{cases} \tag{30}$$

$$N_{i,p}(\xi) = \frac{\xi - \xi_i}{\xi_{i+p} - \xi_i} N_{i,p-1}(\xi) + \frac{\xi_{i+p+1} - \xi}{\xi_{i+p+1} - \xi_{i+1}} N_{i+1,p-1}(\xi) \tag{31}$$

4.2. Univariate NURBS basis functions

The univariate Non-Uniform Rational B-spline (NURBS) can describe objects that cannot be represented by polynomial basis, such as circular arcs. NURBS are built from B-splines by dividing each B-spline basis functions by a weight function

$$W(\xi) = \sum_{j=1}^{n} w_j N_{j,p} \tag{32}$$

and multiplying each B-spline basis functions by the associated weight coefficient for the partition of unity. Thus, the NURBS basis functions are defined as:

$$R_{i,p}(\xi) = \frac{w_i N_{i,p}}{W(\xi)} \tag{33}$$

4.3. Multivariate basis functions

For higher dimensional spaces, the B-spline and NURBS basis functions can be formed by the Kronecker product of vectors of univariate basis functions. For a two-dimensional parametric space, given polynomial orders of p_ξ, p_η and degrees of freedom n_ξ, n_η in ξ, η direction, the bivariate B-spline basis functions are defined as:

$$N_{a,\mathbf{p}}(\xi, \eta) = N_{i,p_\xi}(\xi) N_{j,p_\eta}(\eta), \tag{34}$$

17

where the index a is defined by the map

$$a = n_\eta i + j. \tag{35}$$

The bivariate NURBS basis functions are defined as

$$R_{a,\mathbf{p}}(\xi, \eta) = \frac{w_a N_{a,\mathbf{p}}}{\sum_{i=1}^{n} w_i N_{i,\mathbf{p}}}, \tag{36}$$

where $n = n_\xi \times n_\eta$. With some abuse of notation, we will drop the dependency on the polynomial oder and use N_i to denote both NURBS basis functions and B-spline basis functions in the rest of the paper.

5. Weak-C^1 coupling for two-patch planar domains

To ground our approach in a practical example, we consider a biharmonic problem on a two-patch planar domain, as demonstrated in Figure. 4. The domain Ω is decomposed to the slave subdomain Ω_s (with finer mesh on the interface) and the master subdomain Ω_m (with coarser mesh on the interface).

In order of focusing on the coupling algorithm itself, we assume the boundaries that neighboring to the common intersection to be homogeneous Neumann boundaries (north and south of Ω_s and east and west of Ω_m) and the rest to be homogeneous Dirichlet boundaries (west of Ω_s and south of Ω_m), denoted by Γ_N and Γ_D respectively. Then, the strong form of the two-patch biharmonic boundary value problem writes:

$$
\begin{aligned}
\Delta^2 u &= f, &&\text{in } \Omega, \\
u = \frac{\partial u}{\partial \mathbf{n}} &= 0, &&\text{on } \Gamma_D, \\
\Delta u = \frac{\partial \Delta u}{\partial \mathbf{n}} &= 0, &&\text{on } \Gamma_N.
\end{aligned}
\tag{37}
$$

5.1. Continuity constraints

The weak solution of the biharmonic problem (37) is in the space $H^2(\Omega)$. Due to the inclusion $C^1(\Omega) \subset H^2(\Omega)$, we can use C^1-continuous functions to approximate the solution. For the two multi-patch domain, constraints
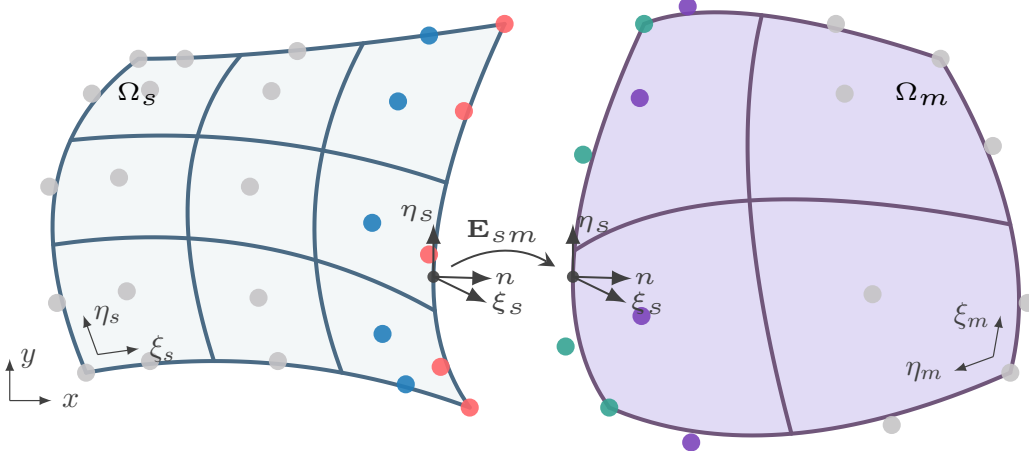
18

Figure 4: A two-patch planar domain constituted by Ω_m and Ω_s.

should be added to compromise the discontinuity along the intersection. In general, the following two constraints are requested for u to be C^1-continuous

$$[u]_{\Gamma_{sm}} = 0, \tag{38a}$$

$$[\frac{\partial u}{\partial \mathbf{n}}]_{\Gamma_{sm}} = 0, \quad \text{with } \mathbf{n} = \mathbf{n}_s = -\mathbf{n}_m \tag{38b}$$

where $\mathbf{n}_k$ is the outward normal direction of $\partial\Omega_k$.

Whereas the constraint (38a) can easily fit into the framework of dual mortar method, the constraint (39) can not be directly imposed. First of all, the existence of dual basis functions of $\frac{\partial N_i}{\partial \mathbf{n}}|_{\Gamma_{sm}}$ is doubtful. Even if they exist, as they are biorthogonal to the normal derivative of NURBS, their formulation must depend on the parameterization of Γ_{sm}, which violates the virtue of simplicity of dual basis functions. Hence, we need the following result, of which the derivatives are defined in the parametric domain and the dual basis functions can be formulated in an elegant manner.

Lemma 1. *Given two differentiable bijective geometric mappings* $\mathbf{F}_s\colon \hat{\Omega}_s \to \Omega_s$ *and* $\mathbf{F}_m\colon \hat{\Omega}_m \to \Omega_m$, *a* C^0-*continuous function* u *is* C^1-*continuous in the physical domain if and only if*

$$[\frac{\partial u}{\partial \xi_s}]_{\Gamma_{sm}} = 0 \ \text{and} \ [\frac{\partial u}{\partial \eta_s}]_{\Gamma_{sm}} = 0. \tag{39}$$

Proof. It suffices to consider two neighboring patches as shown in Figure. 4. u is C^0-continuous function implies $[\frac{\partial u}{\partial \eta_s}]_{\Gamma_{sm}} = 0$. For the C^1-continuity of u,

19

we have the following relation

$$\begin{cases} \frac{\partial u_s}{\partial x} = \frac{\partial u_m}{\partial x} \\ \frac{\partial u_s}{\partial y} = \frac{\partial u_m}{\partial y} \end{cases} \xleftrightarrow{[\frac{\partial u}{\partial \eta_s}]_{\Gamma_{sm}}=0} \begin{cases} \frac{\partial u_s}{\partial \xi_s} \frac{\partial \xi_s}{\partial x} = \frac{\partial u_m}{\partial \xi_s} \frac{\partial \xi_s}{\partial x} \\ \frac{\partial u_s}{\partial \xi_s} \frac{\partial \xi_s}{\partial y} = \frac{\partial u_m}{\partial \xi_s} \frac{\partial \xi_s}{\partial y} \end{cases} \quad \text{on } \Gamma_{sm} \qquad (40)$$

Since the geometric mapping $\mathbf{F}_s$ is bijective, there exist an inverse mapping $\mathbf{F}_s^{-1}$ and $\det(\mathbf{F}_s^{-1}) \neq 0$. Thus, $[\frac{\partial u}{\partial \xi_s}]_{\Gamma_{sm}} = 0$. This concludes the proof. $\qquad \square$

The derivatives of u_m w.r.t. ξ_s and η_s can be obtained following the chain rule, as

$$\begin{bmatrix} \frac{\partial u_m}{\partial \xi_s} \\ \frac{\partial u_m}{\partial \eta_s} \end{bmatrix} = J(\mathbf{E}_{sm})^T \cdot \begin{bmatrix} \frac{\partial u_m}{\partial \xi_m} \\ \frac{\partial u_m}{\partial \eta_m} \end{bmatrix}, \qquad (41)$$

where $J(\cdot)$ is the Jacobian of the mapping in the argument. The Jacobian of the composition mapping $\mathbf{E}_{sm}$ can be written as

$$J(\mathbf{E}_{sm}) = J((\mathbf{F}_m)^{-1} \circ \mathbf{F}_s) = J((\mathbf{F}_m)^{-1}) \cdot J(\mathbf{F}_s) = J(\mathbf{F}_m)^{-1} \cdot J(\mathbf{F}_s). \qquad (42)$$

5.2. Lagrange multiplier formulation and dual mortar formulation

We introduce two Lagrange multiplier spaces: M_0 is devoted to the C^0 constraint (38a) and M_1 is devoted to the C^1 constraint (39). The Lagrange multiplier formulation of the weak problem of (37) reads: find $u \in X_b$, $\lambda_0 \in M_0$ and $\lambda_1 \in M_1$ such that:

$$\begin{cases} a_b(u, v) + b_0(\lambda_0, v) + b_1(\lambda_1, v) = l(v), \quad \forall v \in X_b; \\ b_0(\mu_0, u) = 0, \quad \forall \mu_0 \in M_0; \\ b_1(\mu_1, u) = 0, \quad \forall \mu_1 \in M_1; \end{cases} \qquad (43)$$

with

$$a_b(u, v) = \int_\Omega \Delta u \Delta v d\Omega, \qquad (44)$$

$$b_0(\mu, u) = \int_{\Gamma_{sm}} \mu \, [u]_\Gamma \, d\Gamma, \qquad (45)$$

$$b_1(\mu, u) = \int_{\Gamma_{sm}} \mu \left[\frac{\partial u}{\partial \xi_s} \right]_\Gamma d\Gamma. \qquad (46)$$

The broken Sobolev space for the biharmonic problem is given as

$$\mathcal{X}_b := \left\{ u \in L^2(\Omega) : u|_{\Omega_k} \in H^2_*(\Omega_k) \right\}, \qquad (47)$$

20

with

$$H_*^2(\Omega_k) := \left\{ u \in H^2(\Omega_k) : u = 0 \text{ and } \frac{\partial u}{\partial \mathbf{n}} = 0 \quad \text{on } \partial\Gamma_D \bigcap \partial\Omega_k \right\}. \quad (48)$$

By moving the constraints from the problem statement to the definition of the trial and test function spaces, we obtain the following variational problem: find $u \in \mathcal{K}_b$, such that

$$a_b(u, v) = l(v), \quad \forall v \in \mathcal{K}_b, \quad (49)$$

where

$$\mathcal{K}_b := \{ u \in \mathcal{X}_b : b_0(u, \mu_0) = 0 \text{ and } b_1(u, \mu_1) = 0 \quad \forall(\mu_0, \mu_1) \in \mathcal{M}_0 \times \mathcal{M}_1 \}. \quad (50)$$

On one hand, the absence of the Lagrange multipliers λ_0 and λ_1 reduces the size of the discretized problem and recovers the symmetric positive definite structure of the stiffness matrix. As a result, efficient iterative solvers can be applied for the problem. On the other hand, in the standard formalism, $\mathcal{M}_0$ and $\mathcal{M}_1$ are discretized by the trace of one side of the intersection so that the construction of $\mathcal{K}_b^h$ requires a factorization of a global constraint matrix, which is not a trivial task.

However, in the following section, we will show that, with the help of dual basis functions, the discretized function space $\mathcal{K}_b^h$ can be formulated in an elegant manner.

5.3. Finite element approximation

Suppose that $\mathcal{X}_b^h \subset \mathcal{X}_b$, $\mathcal{M}_0^h \subset \mathcal{M}_0$ and $\mathcal{M}_1^h \subset \mathcal{M}_1$ are finite-dimensional linear subspaces of the Hilbert spaces $\mathcal{X}_b$, $\mathcal{M}_0$, and $\mathcal{M}_1$; we study the finite element approximation of the abstract problem (43).

Assumption 1. *All bilinear functionals are bounded; i.e., there exist positive constants C_a, C_{b_0} and C_{b_1} such that*

$$\begin{aligned} |a_b(u, v)| &\leq C_a \|u\|_{H^2} \|v\|_{H^2} & \forall u, v \in \mathcal{X}_b \\ |b_0(\mu_0, u)| &\leq C_{b_0} \|\mu_0\|_{L^2} \|v\|_{H^2} & \forall \mu_0 \in \mathcal{M}_0, u \in \mathcal{X}_b \quad (51) \\ |b_1(\mu_1, u)| &\leq C_{b_1} \|\mu_1\|_{L^2} \|v\|_{H^2} & \forall \mu_1 \in \mathcal{M}_1, u \in \mathcal{X}_b \end{aligned}$$

Assumption 2. *In addition, we assume that the bilinear functional $a_b(\cdot, \cdot)$ is coercive on $\mathcal{K}_b$, i.e.,*

$$\exists c_a > 0 \quad s.t. \quad \forall v^h \in \mathcal{K}_b^h, \quad a_b(v^h, v^h) \geq c_a \|v^h\|_{H^2} \quad (52)$$

21

Following standard techniques [20], we now obtain a bound on the error between u and u^h in term of the best approximation errors, which can be considered as Céa's lemma for mixed problems.

Theorem 1. *Under the above assumptions, there exsits a unique solution $u^h \in \mathcal{K}_b^h$ satisfies (49). Furthermore,*

$$\|u - u^h\|_{H^2} \leq \left(1 + \frac{C_a}{c_a}\right) \inf_{v^h \in \mathcal{K}_b^h} \|u - u^h\|_{H^2} + \frac{C_{b_0}}{c_a} \inf_{\mu_0^h \in \mathcal{M}_0^h} \|\lambda_0 - \mu_0^h\|_{L^2} + \frac{C_{b_1}}{c_a} \inf_{\mu_1^h \in \mathcal{M}_1^h} \|\lambda_1 - \mu_1^h\|_{L^2} \tag{53}$$

Hence, the error of finite element approximations in broken $H^2(\Omega)$ norm are bounded by the best approximation error of $v^h \in \mathcal{K}_b^h$ in broken $H^2(\Omega)$ norm and $\mu_0^h \in \mathcal{M}_0^h$, $\mu_1^h \in \mathcal{M}_1^h$ in $L^2(\Gamma)$ norm. In general, the approximation ability of pth order piecewise polynomial in $\mathcal{X}_b^h$ is given by

$$\|u - u^h\|_{H^2} \leq Ch^{p-1}. \tag{54}$$

where C is a constant that is independent of the mesh size h. However, the optimality of $u^h \in \mathcal{K}_b^h$ requires the *inf-sup* stability of bilinear functional b_0 and b_1. The analytical study of the *inf-sup* stability is beyond the scope of this paper. Instead, we demonstrate the approximation ability of $\mathcal{K}_b^h$ by directly conducting H^2 projection in different numerical examples.

Meanwhile, the approximation ability of the Lagrange multiplier spaces $\mathcal{M}_0^h$ and $\mathcal{M}_1^h$ also influence the optimality of the finite element approximation. Whereas u is approximated in H^2 space, λ_0 and λ_1 are approximated in L^2 space. Hence, the optimality of the finite element approximation is obtained if both $\mathcal{M}_0^h$ and $\mathcal{M}_1^h$ are $p - 2$ complete, i.e., functions in $\mathcal{M}_0^h$ and $\mathcal{M}_1^h$ can exactly represent polynomials up to order $p - 2$.

5.4. Discretization

In order to approximate the solution of the variational problem, we use the NURBS basis functions $N_i^{(s)}$ $i \in I_s$ and $N_j^{(m)}$ $j \in I_m$ to discretize coupled patches Ω_s and Ω_m, respectively. An appropriate offset has been made so that there is no overlapping between index sets I_s and I_m (given n_s basis functions in Ω_s, we can assume the starting index in the index set I_m is

22

$n_s + 1$). The discretized geometrical mappings are represented by

$$\mathbf{F}_s = \sum_{i \in I_s} \mathbf{P}_i^s N_i^s, \tag{55}$$

$$\mathbf{F}_m = \sum_{i \in I_m} \mathbf{P}_i^m N_i^m, \tag{56}$$

where the control points $\mathbf{P}_i^s, \mathbf{P}_i^m \in \mathbb{R}^2$. The same basis functions are also used to discretize the test function u in broken Sobolev space $\mathcal{X}_b$, as

$$u^h = \sum_{i \in I_s + I_m} U_i N_i, \tag{57}$$

with

$$N_i = \begin{cases} N_i^s, & i \in I_s; \\ N_i^m, & i \in I_m. \end{cases} \tag{58}$$

As compared to the standard formalism that utilizes the trace of the slave patch on the intersection as the discretization of Lagrange multipliers, in this research, we construct Lagrange multipliers by using Bézier dual basis. We first classify NURBS basis functions into five different kinds, as shown in Figure. 4, namely:

1. The basis functions $N_i^{(s)}$ such that $\mathrm{supp}(N_i^{(s)}) \bigcap \Gamma_{sm} = \emptyset$ and $\mathrm{supp}(\frac{\partial N_i^{(s)}}{\partial \xi_s}) \bigcap \Gamma_{sm} \neq \emptyset$, whose indices are in the index set I_i. (denoted by blue dots)

2. The basis functions $N_i^{(s)}$ such that $\mathrm{supp}(N_i^{(s)}) \bigcap \Gamma_{sm} \neq \emptyset$, whose indices are in the index set I_{ii}. (denoted by red dots)

3. The basis functions $N_i^{(m)}$ such that $\mathrm{supp}(N_i^{(m)}) \bigcap \Gamma_{sm} = \emptyset$ and $\mathrm{supp}(\frac{\partial N_i^{(m)}}{\partial \xi_s}) \bigcap \Gamma_{sm} \neq \emptyset$, whose indices are in the index set I_{iii}. (denoted by green dots)

4. The basis functions $N_i^{(m)}$ such that $\mathrm{supp}(N_i^{(m)}) \bigcap \Gamma_{sm} \neq \emptyset$, whose indices are in the index set I_{iv}. (denoted by purple dots)

5. All basis functions neither the supports of themselves nor the supports of their first order derivatives in ξ_s direction intersect with Γ_{sm}, whose indices are in the index set I_v. (denoted by grey dots)

For the basis functions of the second kind, their restrictions on the intersection Γ_{sm} are one dimensional NURBS basis functions $N_{i,p_\eta}^{(s)}$ $i \in \{1, 2, \ldots, n_\eta^s\}$ that are used to discretize the tensor-product domain Ω_s in η direction. In

23

order to obtain an Identity matrix on the slave side of the discretized bilinear form b_0, the associated dual basis functions of $N_{i,p_\eta}^{(s)}$ are used to discretize the Lagrange multiplier space $\mathcal{M}_0$, as

$$\lambda_0^h = \sum_{i=1}^{n_\eta^s} \Lambda_i^0 \hat{N}_{i,p_\eta}^{(s)}. \tag{59}$$

For the basis functions of the first kind, the restrictions of their first order derivatives on the intersection Γ_{sm} can be written as $cN_{i,p_\eta}^{(s)}$ $i \in \{1, 2, \ldots, n_\eta^s\}$, with $c = N_{n_\xi^s-1,p_\xi}^{(s)}{}'(1)$. Hence, the Lagrange multiplier space $\mathcal{M}_1$ can be discretized by

$$\lambda_1^h = \sum_{i=1}^{n_\eta^s} \Lambda_i^1 \tilde{N}_i, \quad \text{with } \tilde{N}_i = \frac{1}{c} N_{i,p_\eta}^{(s)}. \tag{60}$$

We denote the basis functions in $\mathcal{M}_0^h$ and $\mathcal{M}_1^h$ as the dual basis functions of the second and the first kinds of NURBS basis functions, respectively.

By substituting these NURBS approximations into the Lagrange multiplier formulation (43), we obtain the following linear system:

$$\begin{bmatrix} \mathbf{K} & \mathbf{B}^T \\ \mathbf{B} & \mathbf{0} \end{bmatrix} \begin{bmatrix} \mathbf{U} \\ \mathbf{\Lambda_0} \\ \mathbf{\Lambda_1} \end{bmatrix} = \begin{bmatrix} \mathbf{F} \\ \mathbf{0} \end{bmatrix}, \tag{61}$$

where $\mathbf{K}$ and $\mathbf{F}$ are the stiffness matrix and the load vector for the uncoupled problem, respectively. $\mathbf{B}$ is the constraint matrix discretized from the bilinear forms b_0 and b_1. In order to construct the finite element space $\mathcal{K}_b^h$, we need to solve the constraint matrix $\mathbf{B}$'s null space $\mathbf{C} = \ker(\mathbf{B})$. Since the structure of the constraint matrix $\mathbf{B}$ depends on the index sets I_s and I_m and the ordering of Lagrange multiplier basis functions, without adding any constraints on the indices, we introduce two permutation matrices $\mathbf{P}_c$ and $\mathbf{P}_r$ (this step is not neccessary from the implementation point of view, but is very convenient for the demonstration, especially for multi-patch problem). We define the column permutation matrix $\mathbf{P}_c$ as

$$\begin{bmatrix} \mathbf{I}_i \\ \mathbf{I}_{ii} \\ \mathbf{I}_{iii} \\ \mathbf{I}_{iv} \\ \mathbf{I}_v \end{bmatrix} = \mathbf{P}_c \begin{bmatrix} \mathbf{I}_s \\ \mathbf{I}_m \end{bmatrix}, \tag{62}$$

24

where $\mathbf{I}_i$ is the vector form of the index set I_i. For an appropriate row permutation matrix $\mathbf{P}_r$, the modified constraint matrix can be written in a partitioned form as

$$\mathbf{B}_p = \mathbf{P}_r \mathbf{B} \mathbf{P}_c^T = \begin{bmatrix} \mathbf{B}_1^1 & \mathbf{B}_1^2 & \mathbf{B}_1^3 & \mathbf{B}_1^4 & \mathbf{0} \\ \mathbf{0} & \mathbf{B}_2^2 & \mathbf{B}_2^3 & \mathbf{0} & \mathbf{0} \end{bmatrix}, \tag{63}$$

where $\mathbf{B}_i^j$ corresponds to the contribution of the inner product of the basis functions of the jth kind with the dual basis functions of the ith kind. $\mathbf{P}_r$ can be defined as a row permutation matrix such that the resulted block sub-matrices $\mathbf{B}_1^1$ and $\mathbf{B}_2^2$ are both identity matrices. Under a rank-preserving transformation $\mathbf{T}$, we can eliminate the block sub-matrix $\mathbf{B}_1^2$, as

$$\mathbf{T}\mathbf{B}_p = \begin{bmatrix} & \mathbf{I} & & \mathbf{B}_1^3 - \mathbf{B}_1^2\mathbf{B}_2^3 & \mathbf{B}_1^4 & \mathbf{0} \\ & & & \mathbf{B}_2^3 & \mathbf{0} & \mathbf{0} \end{bmatrix}. \tag{64}$$

We may now take

$$\mathbf{C}_p := \ker(\mathbf{B}_p) = \begin{bmatrix} \mathbf{B}_1^2\mathbf{B}_2^3 - \mathbf{B}_1^3 & -\mathbf{B}_1^4 & \mathbf{0} \\ -\mathbf{B}_2^3 & \mathbf{0} & \mathbf{0} \\ \hdashline & \mathbf{I} & \end{bmatrix}. \tag{65}$$

Hence, the null space of $\mathbf{B}$ can be taken as

$$\mathbf{C} = \mathbf{P}_c^T \mathbf{C}_p. \tag{66}$$

Now we can discretize functions in $\mathcal{K}_b^h$ as

$$u^h = \mathbf{N}^T \mathbf{U}, \quad \text{with } \mathbf{U} = \mathbf{C}\tilde{\mathbf{U}}, \tag{67}$$

where $\mathbf{N}$ is the vector form of basis functions of $\mathcal{X}_b^h$, and $\tilde{\mathbf{U}}$ is the control point vector. By substituting the above discretization in the weak form (50), we obtain the following linear system to be solved:

$$\mathbf{C}^T \mathbf{K} \mathbf{C} \tilde{\mathbf{U}} = \mathbf{C}^T \mathbf{F}. \tag{68}$$

Because of the biorthogonality of the NURBS basis functions and their dual basis functions, the constrained solution spcae $\mathcal{K}_b^h$ can be constructed very efficiently, leading to a sparse, symmetric positive definite formulation.
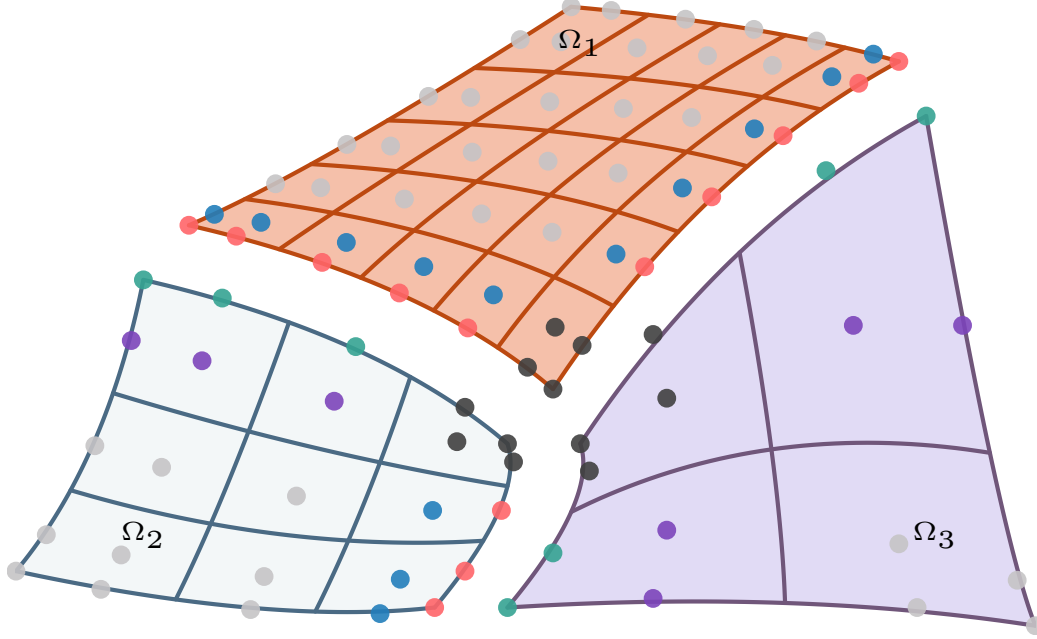
Figure 5: A three-patch planar domain constituted by Ω_1, Ω_2 and Ω_3.

6. Weak-C^1 coupling for multi-patch planar domains

To generate complex geometries, we need to decompose domain to multiple patches. Unfortunately, we cannot apply directly the results of two-patch coupling to this more general mortar situation. The main issue is the so-called cross points. For a multi-patch decomposition, at least three subdomains meet at an interior crosspoint and several interfaces can share this cross point as a common endpoint (Figure. 5). If we use the discretized Lagrange multipliers proposed in the previous section, owing to the presence of cross points, some of the control points will serve as both slave points (indices in I_1 and I_2) and master points (indices in I_3 and I_4). Hence, there is no permutation matrices such that the constraint matrix $\mathbf{B}$ can be modified to the form as equation (64), of which the null space can be found in a trivial way. Even more, although the constraint matrices defined on each interfaces are full row rank, the assembled constraint matrix $\mathbf{B}$ may not be full row rank in most cases, which renders the linear system (61) to be rank deficient. As a result, either modifications to the Lagrange multipliers or to the method itself is required so that the proposed method can be generalized to a setting where a domain can be decomposed to an arbitrary number of

26

patches. Before we start this section, we would like to introduce the sixth kind of NURBS basis function that associated with the cross point v, as

6. The basis function N_i such that $\text{supp}(N_i) \bigcap v \neq 0$, or $\text{supp}(\frac{\partial N_i}{\partial \xi}) \bigcap v \neq 0$, or $\text{supp}(\frac{\partial N_i}{\partial \eta}) \bigcap v \neq 0$ or $\text{supp}(\frac{\partial^2 N_i}{\partial \xi \partial \eta}) \bigcap v \neq 0$, whose indices are in the index set I_{vi}. (denoted by black dots in Figure. 5)

The rest five kinds of NURBS basis function remain the same except their intersection with the sixth kind are excluded, that is

$$I_k = I_k - I_{vi} \bigcap I_k, \quad k \in \{i, ii, \ldots, v\}. \tag{69}$$

The basis functions in $\mathcal{M}_0^h$ and $\mathcal{M}_1^h$ can be classified as the dual basis functions of the NURBS basis function of the 1st, 2nd and 6th kind, respectively. The domains on the two sides of each interface can still be considered as slave and master based on the same rule as for the two-patch coupling case.

6.1. Cross point modification

Since using the discretization of Lagrange multipliers proposed for two-patch coupling case directly results in over-constrained constraint matrix $\mathbf{B}$ for the control points round the crosspoints, we can remedy this issue by reducing the dimension of the Lagrange multiplier spaces. Roughly speaking, we have to remove the two degrees of freedom of the Lagrange multiplier spaces associated with each cross point so that the resulted Lagrange multiplier spaces on each interface should have the same dimension as $\mathcal{X}_b^h|_{\Omega_s} \bigcap H_0^2(\Gamma_{sm})$.

This can be achieved by two ways: we can either coarse the mesh for the Lagrange multiplier in the neighborhood of the cross point, or reduce their polynomial degree in the neighborhood of the cross point. An example for quadratic 1-D B-spline basis functions is shown in Figure. 6. The coarsed basis functions are achieved by replacing the first three and last three basis functions by their summations, while we can construct degree reduced basis functions by reduce the polynomial degree of the first and last two elements by one while retaining the inter-element continuity.

Although the degree reduction is not a trivial task for dual basis, the summation trick can be applied to coarse dual basis functions. After the coarsen procedure, the dual basis functions associated with the basis functions of 6th kind are all eliminated so that no inter-dependencies will happen
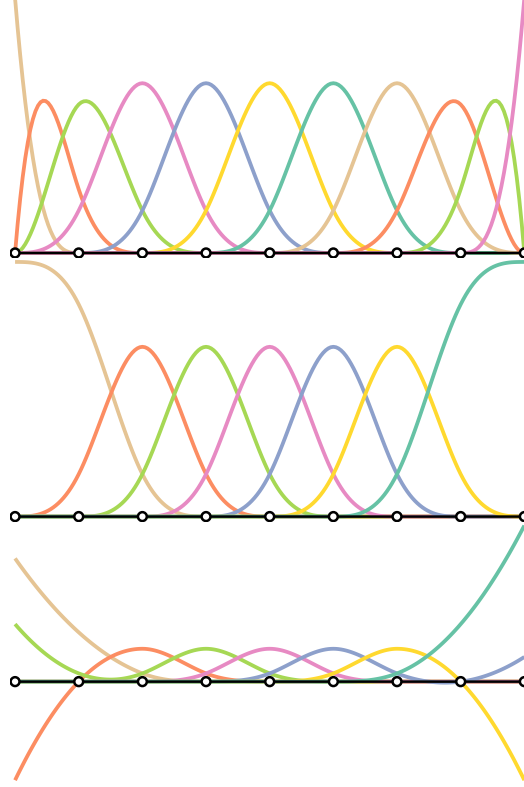
27

Figure 6: Quadratic basis functions and their cross point modifications. Top: original quadratic basis functions. Middle: coarsed basis functions. Bottom: degree reduced basis functions

in the neighborhood of the cross point. We can define a column permutation matrix

$$
\begin{bmatrix} \mathbf{I}_i \\ \mathbf{I}_{ii} \\ \mathbf{I}_{iii} \\ \mathbf{I}_{iv} \\ \mathbf{I}_{vi} \\ \mathbf{I}_v \end{bmatrix} = \tilde{\mathbf{P}}_c \begin{bmatrix} \mathbf{I}_1 \\ \mathbf{I}_2 \\ \mathbf{I}_3 \end{bmatrix}. \tag{70}
$$

With a suitable row permutation matrix $\tilde{\mathbf{P}}_r$, the constraint matrix $\mathbf{B}$ can be modified as

$$
\tilde{\mathbf{B}}_p := \tilde{\mathbf{P}}_r \mathbf{B} \tilde{\mathbf{P}}_c^T = \begin{bmatrix} \mathbf{B}_1^1 & \mathbf{B}_1^2 & \mathbf{B}_1^3 & \mathbf{B}_1^4 & \mathbf{B}_1^6 & \mathbf{0} \\ \mathbf{0} & \mathbf{B}_2^2 & \mathbf{B}_2^3 & \mathbf{0} & \mathbf{B}_2^6 & \mathbf{0} \end{bmatrix}, \tag{71}
$$

28

with $\mathbf{B}_1^1$ and $\mathbf{B}_2^2$ be identity matrices. Hence, its null space can be found as

$$\tilde{\mathbf{C}}_p := \ker(\tilde{\mathbf{B}}_p) = \begin{bmatrix} \mathbf{B}_1^2\mathbf{B}_2^3 - \mathbf{B}_1^3 & -\mathbf{B}_1^4 & -\mathbf{B}_1^6 & \mathbf{0} \\ -\mathbf{B}_2^3 & \mathbf{0} & -\mathbf{B}_2^6 & \mathbf{0} \\ \hdashline & \mathbf{I} & \end{bmatrix}. \tag{72}$$

Although the boundary modification by coarsening eliminates the inter-dependency in the neighborhood of cross points, numerical tests demonstrate sub-optimality.

6.2. Explicitly solve the null space

Instead of modifying the Lagrange multipliers, we can solve the null space of the over-constrained constraint matrix $\mathbf{B}$ directly. Seveal matrix factorization methods can be used to solve the null space, including LU, QR, SVD. For example, a rank-revealing QR factorization over a rank-deficiency constraint matrix $\mathbf{B}$ yields

$$\mathbf{B}\mathbf{P} = \mathbf{Q}\begin{bmatrix} \mathbf{R}_1 & \mathbf{R}_2 \\ \mathbf{0} & \mathbf{0} \end{bmatrix} \tag{73}$$

where $\mathbf{P}$ is a permutation matrix, $\mathbf{Q}$ is an unitary matrix, $\mathbf{R}_1$ is a upper triangular matrix and $\mathbf{R}_2$ is a rectangular matrix. The null space can be taken as

$$\ker(\mathbf{B}) = \mathbf{P}\begin{bmatrix} -\mathbf{R}_1^{-1}\mathbf{R}_2 \\ \mathbf{I} \end{bmatrix}. \tag{74}$$

However, this requires a factorization of the entire constraint matrix $\mathbf{B}$ and we fail to utilize the advantage of the Bézier dual basis. Even more, the sparsity of the constrained stiffness matrix might be impacted as the inverse of $\mathbf{R}_1$ is a dense matrix. This type of global factorization has been utilized for patch coupling problem in [27, 28, 32].

Instead of solving the null space directly, we will localize the constraint to each cross point and solve the null space of a localized linear system. For the constraint matrix $\mathbf{B}$ constructed by the Lagrange multipliers without modification, we assume there exist a row permutation matrix $\hat{\mathbf{P}}_r$ such that

$$\hat{\mathbf{B}}_p := \hat{\mathbf{P}}_r\mathbf{B}\tilde{\mathbf{P}}_c^T = \begin{bmatrix} \mathbf{B}_1 \\ \hdashline \mathbf{B}_2 \end{bmatrix} = \begin{bmatrix} \mathbf{B}_6^1 & \mathbf{B}_6^2 & \mathbf{B}_6^3 & \mathbf{B}_6^4 & \mathbf{B}_6^6 & \mathbf{0} \\ \hdashline \mathbf{B}_1^1 & \mathbf{B}_1^2 & \mathbf{B}_1^3 & \mathbf{B}_1^4 & \mathbf{B}_1^6 & \mathbf{0} \\ \mathbf{0} & \mathbf{B}_2^2 & \mathbf{B}_2^3 & \mathbf{0} & \mathbf{B}_2^6 & \mathbf{0} \end{bmatrix}, \tag{75}$$

with $\mathbf{B}_1^1$ and $\mathbf{B}_2^2$ be identity matrices. $\mathbf{B}_1$ consists of constraints relevant to cross point while $\mathbf{B}_2$ consists of constraints relevant to intersections.

29

The null space of $\mathbf{B}_2$ can be found as

$$\mathbf{C}_2 := \ker(\mathbf{B}_2) = \left[\begin{array}{c} \begin{array}{cccc} \mathbf{B}_1^2\mathbf{B}_2^3 - \mathbf{B}_1^3 & -\mathbf{B}_1^4 & -\mathbf{B}_1^6 & \mathbf{0} \\ -\mathbf{B}_2^3 & \mathbf{0} & -\mathbf{B}_2^6 & \mathbf{0} \end{array} \\ \hline \mathbf{I} \end{array} \right]. \qquad (76)$$

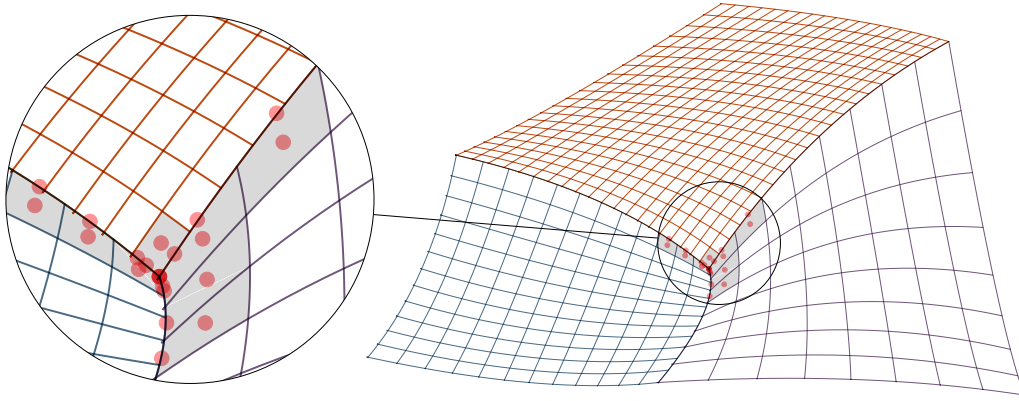Due to the inclusion $\hat{\mathbf{C}}_p := \ker(\hat{\mathbf{B}}_p) \subset \ker(\mathbf{B}_2)$, we can construct $\hat{\mathbf{C}}_p$ by

Figure 7: Control points (red) involved in crosspoint constraints ($\mathbf{B}_1$).

solving $\ker(\mathbf{B}_1\mathbf{C}_2)$. Since dual basis functions have compact support, $\mathbf{B}_1$ and $\mathbf{C}_2$ are all sparse matrices (control points involved in $\mathbf{B}_1$ are demonstrated in Figure. 7). We can split the columns of $\mathbf{C}_2$ into two matrices, as

$$\begin{aligned} \mathbf{C}_2^1 &:= \{v \in \mathbf{C}_2 : \mathbf{B}_1 v \neq 0\}, \\ \mathbf{C}_2^2 &:= \{v \in \mathbf{C}_2 : \mathbf{B}_1 v = 0\}. \end{aligned} \qquad (77)$$

Such a split can be defined a priori, based on the discretization of each patch. A demonstration of the split is givin in Figure. 8. Note that $\mathbf{C}_2^2 \subset \hat{\mathbf{C}}_p$, $\hat{\mathbf{C}}_p$ can be written as

$$\hat{\mathbf{C}}_p = \begin{bmatrix} \mathbf{C}_2^1 \ker(\bar{\mathbf{B}}_p) & \mathbf{C}_2^2 \end{bmatrix}, \text{ with } \bar{\mathbf{B}}_p = \mathbf{B}_1\mathbf{C}_2^1. \qquad (78)$$

Compared with the constraint matrix $\mathbf{B}$ whose size increases as we refine the mesh, the row size of $\bar{\mathbf{B}}_p$ is fixed and its column size is fixed after certain refinement. A comparison of the size of matrix $\mathbf{B}$ and matrix $\bar{\mathbf{B}}_p$ as a function
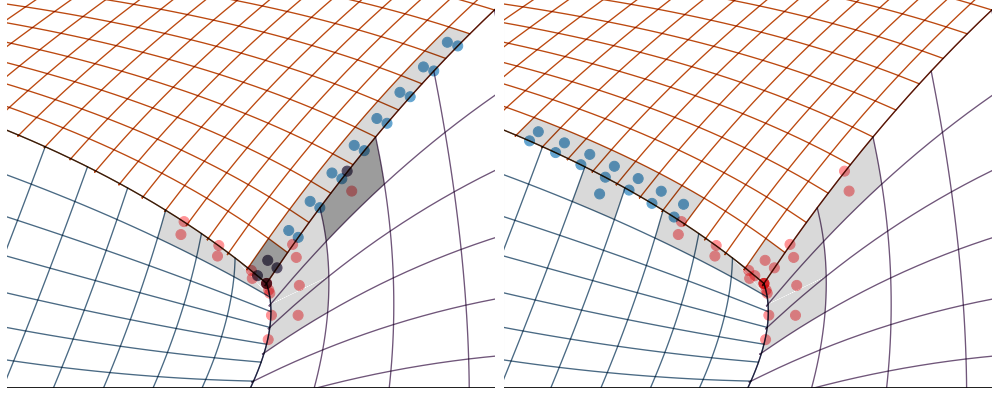
Figure 8: Control points of basis functions (blue) defined by columns of $\mathbf{C}_2$. Left: Basis classified to $\mathbf{C}_2^1$; Right: Basis classified to $\mathbf{C}_2^2$

of the degrees of freedom is given in Figure. 9 for the three-patch coupling in Figure. 5 with 2nd order B-spline basis functions. As can be seen, the size of $\mathbf{B}$ grows rapidly as the mesh being refined. The computational cost of directly solving its kernel will be very expensive. However, owing to the compact support of dual basis function, we can transfer a global, size-varying problem (fractorization on $\mathbf{B}$) to a local, size-fixed problem (factorization on $\bar{\mathbf{B}}_p$), and the problem size is very small (12×24 for this case).

A graphical comparison of the sparity patterns among standard Lagrange multiplier with global factorization, Bézier dual basis with global factorization and Bézier dual basis with local factorization is given in Figure. 10. As expected, the standard method yields the lowest sparsity, while Bézier dual basis with local factorization yields the highest sparsity (40% sparser). Meanwhile, the Bézier dual basis does not significantly improve the sparsity if a global factorization is applied to construct $\mathcal{K}_b^h$. Moreover, a global factorization yeilds entries with very small absolute values ($\leq 10^{-14}$), especially for the constraint matrix formed by Bézier dual basis, while all entries are away from zero for the local factorization.

7. Numerical results

7.1. Biharmonic problem on a two-patch domain with homogeneous Dirichlet Boundary

We first solve a biharmonic problem $\Delta^2 u = f$ on a square domain $\Omega = (0,1) \times (0,1)$. This domain is decomposed into two patches, as shown in
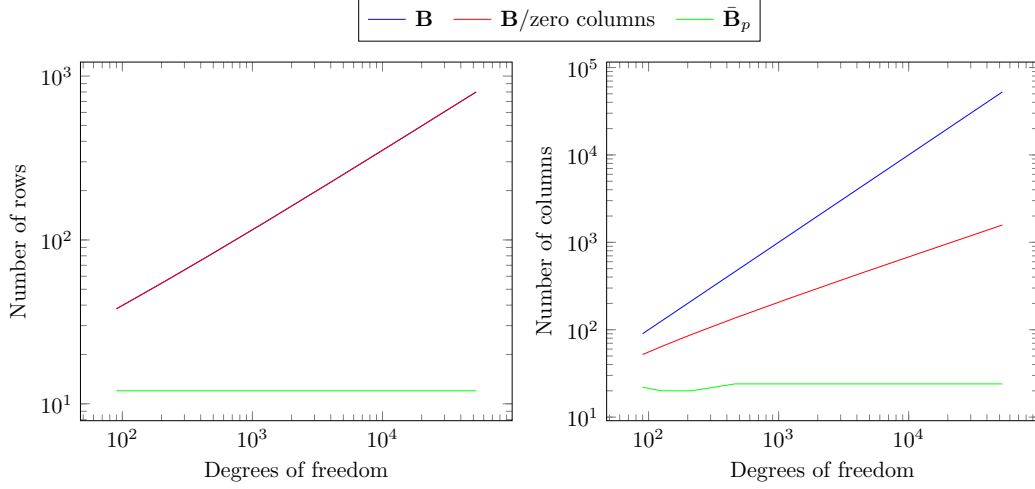
31

Figure 9: The change of matrix size of **B**, **B** with zero columns being removed, and $\bar{\mathbf{B}}_p$, as a function of the degrees of freedom. The constraint matrix **B** is formulated for the three-patch coupling in Figure. 5 with 2nd order B-spline basis functions.

Figure. 11. The manufactrued solution is given as

$$u(x, y) = \sin(\pi x)^2 \sin(\pi y)^2, \tag{79}$$

which satisfies the homogeneous Dirichlet boundary condition ($u = \frac{\partial u}{\partial \mathbf{n}} = 0$) and is visualized in Figure. 11. The right-hand side function f can be obtained by applying the biharmonic operator to u.

8. Schedule

Although there are various aspects in weak C^1/G^1 coupling deserve a thorough study, our main focus in this stage is to extend our finding in an abstract problem (biharmonic problem) to practical problems (e.g. Kirchhoff-Love shell). Compared to the planar biharmonic problem, Kirchhoff-Love shell is a more challenging problem, as the computational domain is in $\mathbb{R}^3$ and the constraint is not isotropically applied in each direction. Hence, a more generalized constraint is needed to compromise geometries with kinks. And validations are needed for two-patch and multi-patch Kirchhoff-Love shells. Meanwhile, although we have implemented two algorithms to solve multi-patch biharmonic problems, the boundary modification method does
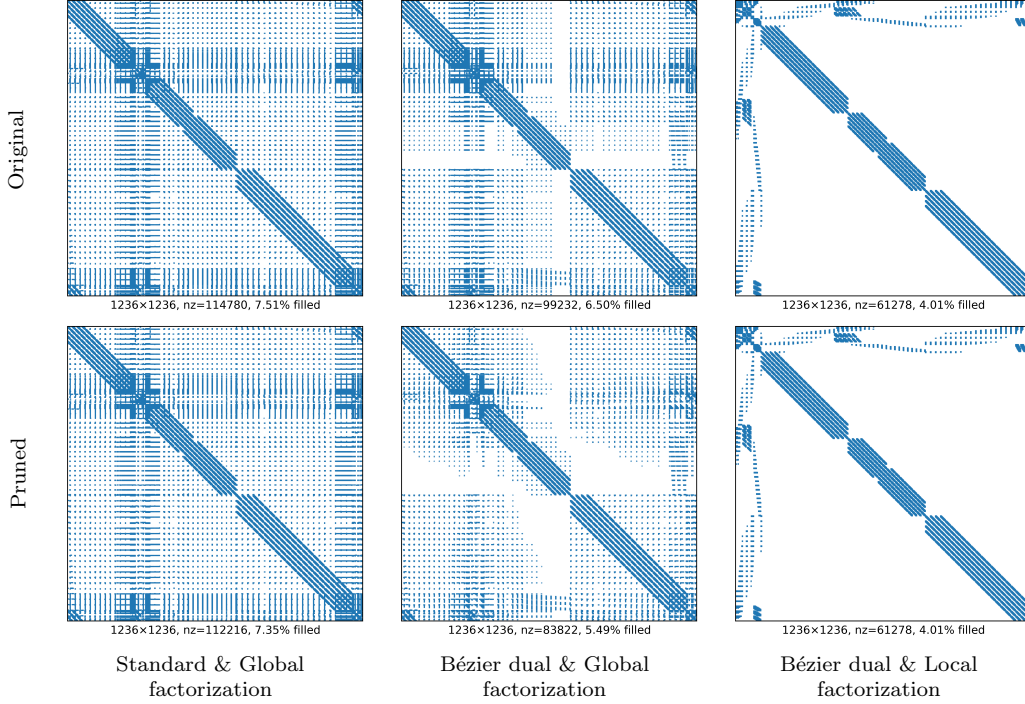
32

Figure 10: Sparsity patterns of constrained stiffness matrices. Left: standard Lagrange multipliers with global factorization. Middle: Bézier dual basis with global factorization. Right: Bézier dual basis with localized factorization. Top: original matrix. Bottom: small absolute values ($\leq 10^{-14}$) be pruned. All stiffness matrices are formulated for the three-patch coupling in Figure. 5 with 3rd order B-spline basis functions after 4 refiments. The number of non-zero entries is given by nz.

not delivers ideal results while an additional factorization is needed for explicitly solving the null space. We will still make efforts in finding a feasible boundary modification for multi-patch coupling. A detailed time line is shown in Table. 2.

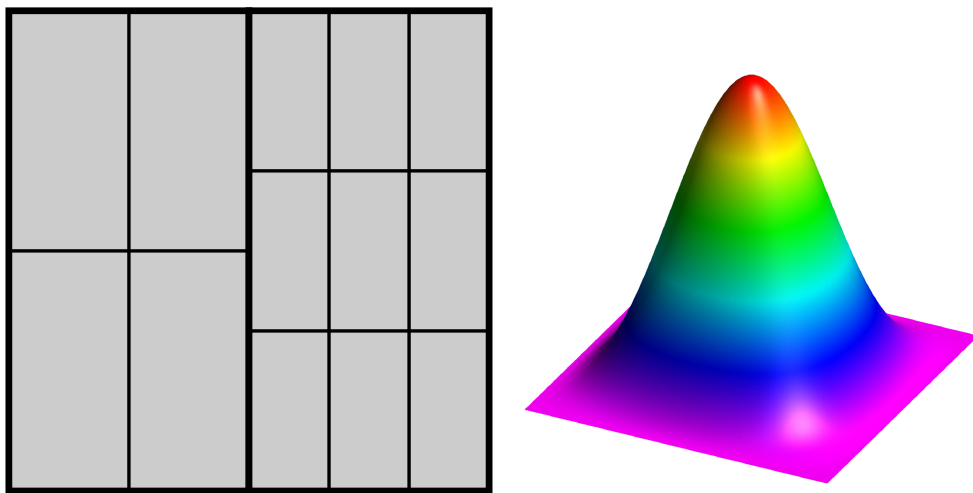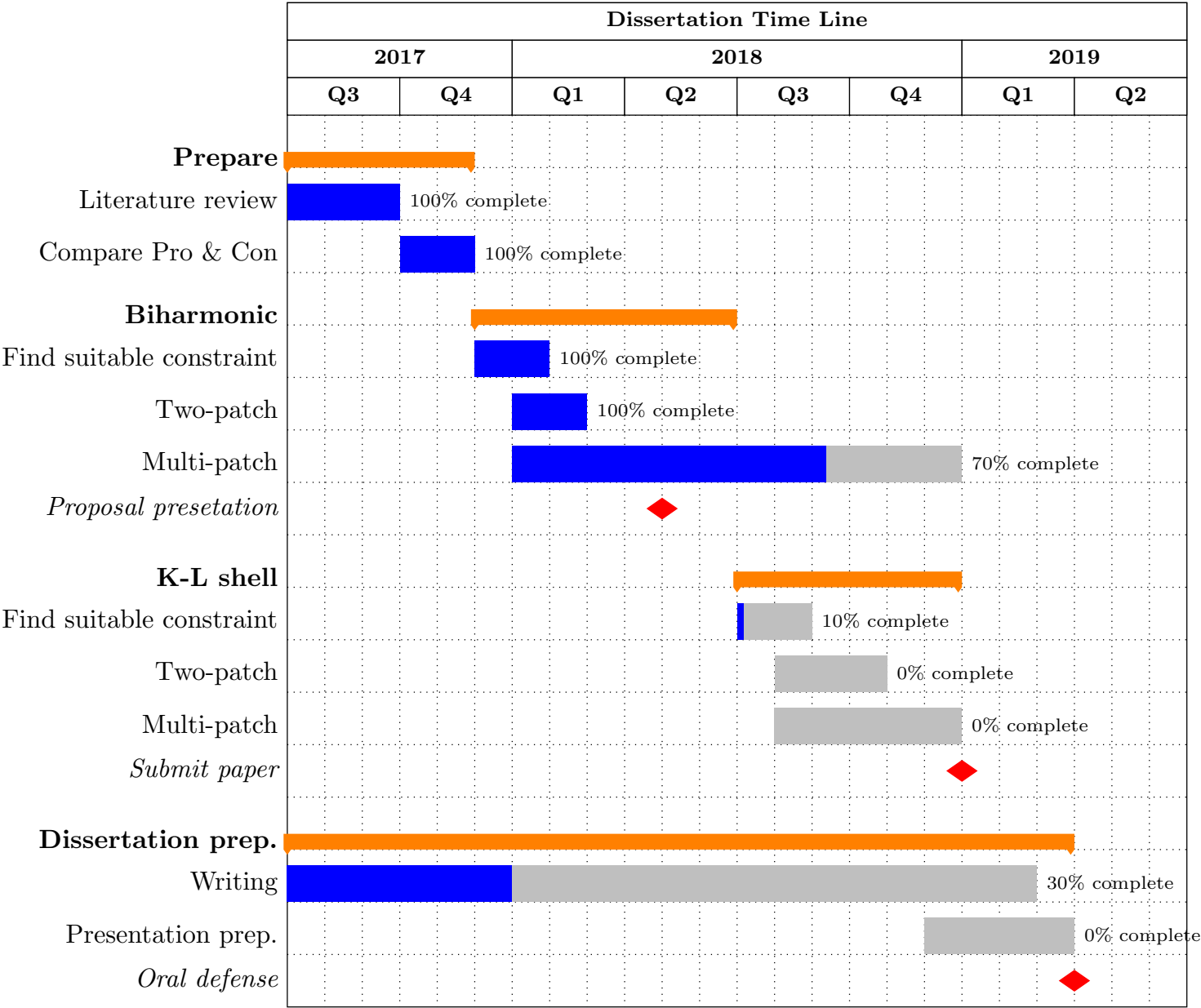Figure 11: The computational domain Ω and the manufactured solution with the property $u = \frac{\partial u}{\partial \mathbf{n}} = 0$ on $\partial\Omega$, which are used in Section 7.1.

Table 2: A schedule of tasks and stages of my research towards the final dissertation.

	Dissertation Time Line							
	2017		2018				2019	
	Q3	Q4	Q1	Q2	Q3	Q4	Q1	Q2

Prepare

Literature review — 100% complete

Compare Pro & Con — 100% complete

Biharmonic

Find suitable constraint — 100% complete

Two-patch — 100% complete

Multi-patch — 70% complete

Proposal presetation

K-L shell

Find suitable constraint — 10% complete

Two-patch — 0% complete

Multi-patch — 0% complete

Submit paper

Dissertation prep.

Writing — 30% complete

Presentation prep. — 0% complete

Oral defense

35

[1] Andreas Apostolatos, Michael Breitenberger, Roland Wüchner, and Kai-Uwe Bletzinger. Domain decomposition methods and kirchhoff-love shell multipatch coupling in isogeometric analysis. In *Isogeometric Analysis and Applications 2014*, pages 73–101. Springer, 2015.

[2] Andreas Apostolatos, Robert Schmidt, Roland Wüchner, and Kai-Uwe Bletzinger. A Nitsche-type formulation and comparison of the most common domain decomposition methods in isogeometric analysis. *International Journal for Numerical Methods in Engineering*, 97(7):473–504, February 2014.

[3] Helio JC Barbosa and Thomas JR Hughes. The finite element method with lagrange multipliers on the boundary: circumventing the babuška-brezzi condition. *Computer Methods in Applied Mechanics and Engineering*, 85(1):109–128, 1991.

[4] Y. Bazilevs, V. M. Calo, J. A. Cottrell, J. A. Evans, T. J. R. Hughes, S. Lipton, M. A. Scott, and T. W. Sederberg. Isogeometric analysis using T-splines. *Computer Methods in Applied Mechanics and Engineering*, 199(5–8):229–263, January 2010.

[5] Yuri Bazilevs, L Beirao da Veiga, J Austin Cottrell, Thomas JR Hughes, and Giancarlo Sangalli. Isogeometric analysis: approximation, stability and error estimates for h-refined meshes. *Mathematical Models and Methods in Applied Sciences*, 16(07):1031–1090, 2006.

[6] Roland Becker, Peter Hansbo, and Rolf Stenberg. A finite element method for domain decomposition with non-matching grids. *ESAIM: Mathematical Modelling and Numerical Analysis - Modélisation Mathématique et Analyse Numérique*, 37(2):209–225, 2003.

[7] F. B. Belgacem, P. Hild, and P. Laborde. The mortar finite element method for contact problems. *Mathematical and Computer Modelling*, 28(4):263–271, August 1998.

[8] Faker Ben Belgacem. The Mortar finite element method with Lagrange multipliers. *Numerische Mathematik*, 84(2):173–197, December 1999.

[9] FAKER BEN BELGACEM, Patrick Hild, and Patrick Laborde. Extension of the mortar finite element method to a variational inequality

modeling unilateral contact. *Mathematical Models and Methods in Applied Sciences*, 9(02):287–303, 1999.

[10] Zakaria Belhachmi and Christine Bernardi. Resolution of fourth-order problems by the mortar element method. *Computer Methods in Applied Mechanics and Engineering*, 116(1):53–58, January 1994.

[11] Michele Benzi and Andrew J. Wathen. Some Preconditioning Techniques for Saddle Point Problems. In Wilhelmus H. A. Schilders, Henk A. van der Vorst, and Joost Rommes, editors, *Model Order Reduction: Theory, Research Aspects and Applications*, number 13 in Mathematics in Industry, pages 195–211. Springer Berlin Heidelberg, 2008. DOI: 10.1007/978-3-540-78841-6_10.

[12] Michel Bercovier and Tanya Matskewich. Smooth Bezier Surfaces over Arbitrary Quadrilateral Meshes. *arXiv:1412.1125 [math]*, December 2014. arXiv: 1412.1125.

[13] C. Bernardi, Y. Maday, and A. T. Patera. Domain Decomposition by the Mortar Element Method. In Hans G. Kaper, Marc Garbey, and Gail W. Pieper, editors, *Asymptotic and Numerical Methods for Partial Differential Equations with Critical Parameters*, pages 269–286. Springer Netherlands, Dordrecht, 1993. DOI: 10.1007/978-94-011-1810-1_17.

[14] Christine Bernardi, Yvon Maday, and Francesca Rapetti. Basics and some applications of the mortar element method. *GAMM-Mitteilungen*, 28(2):97–123, November 2005.

[15] Daniele Boffi, Franco Brezzi, and Michel Fortin. *Mixed Finite Element Methods and Applications*. Springer Series in Computational Mathematics. Springer-Verlag.

[16] Michael J Borden, Thomas JR Hughes, Chad M Landis, and Clemens V Verhoosel. A higher-order phase-field model for brittle fracture: Formulation and analysis within the isogeometric analysis framework. *Computer Methods in Applied Mechanics and Engineering*, 273:100–118, 2014.

[17] Michael J Borden, Clemens V Verhoosel, Michael A Scott, Thomas JR Hughes, and Chad M Landis. A phase-field description of dynamic brit-

tle fracture. *Computer Methods in Applied Mechanics and Engineering*, 217:77–95, 2012.

[18] P. B. Bornemann and F. Cirak. A subdivision-based implementation of the hierarchical b-spline finite element method. *Computer Methods in Applied Mechanics and Engineering*, 253:584–598, January 2013.

[19] Robin Bouclier, Jean-Charles Passieux, and Michel Salaün. Development of a new, more regular, mortar method for the coupling of NURBS subdomains within a NURBS patch: Application to a non-intrusive local enrichment of NURBS patches. *Computer Methods in Applied Mechanics and Engineering*, 316:123–150, April 2017.

[20] Susanne Brenner and Ridgway Scott. *The Mathematical Theory of Finite Element Methods*. Springer Science & Business Media, December 2007. Google-Books-ID: ci4c_R0WKYYC.

[21] Ericka Brivadis, Annalisa Buffa, Barbara Wohlmuth, and Linus Wunderlich. Isogeometric mortar methods. *Computer Methods in Applied Mechanics and Engineering*, 284:292–319, February 2015.

[22] A. Buffa, D. Cho, and G. Sangalli. Linear independence of the T-spline blending functions associated with some particular T-meshes. *Computer Methods in Applied Mechanics and Engineering*, 199(23–24):1437–1445, April 2010.

[23] E. Catmull and J. Clark. Recursively generated B-spline surfaces on arbitrary topological meshes. *Computer-Aided Design*, 10(6):350–355, November 1978.

[24] Franz Chouly, Patrick Hild, and Yves Renard. Symmetric and non-symmetric variants of Nitsche's method for contact problems in elasticity: theory and numerical experiments. *Mathematics of Computation*, 84(293):1089–1112, 2015.

[25] Annabelle Collin, Giancarlo Sangalli, and Thomas Takacs. Analysis-suitable G1 multi-patch parametrizations for C1 isogeometric spaces. *Computer Aided Geometric Design*, 47:93–113, October 2016.

[26] Laurens Coox, Onur Atak, Dirk Vandepitte, and Wim Desmet. An isogeometric indirect boundary element method for solving acoustic problems

38

in open-boundary domains. *Computer Methods in Applied Mechanics and Engineering*, 316:186–208, April 2017.

[27] Laurens Coox, Francesco Greco, Onur Atak, Dirk Vandepitte, and Wim Desmet. A robust patch coupling method for NURBS-based isogeometric analysis of non-conforming multipatch surfaces. *Computer Methods in Applied Mechanics and Engineering*, 316:235–260, April 2017.

[28] Laurens Coox, Florian Maurin, Francesco Greco, Elke Deckers, Dirk Vandepitte, and Wim Desmet. A flexible approach for coupling nurbs patches in rotationless isogeometric analysis of kirchhoff–love shells. *Computer Methods in Applied Mechanics and Engineering*, 325:505–531, 2017.

[29] L Beirao Da Veiga, Annalisa Buffa, Judith Rivas, and Giancarlo Sangalli. Some estimates for h–p–k-refinement in isogeometric analysis. *Numerische Mathematik*, 118(2):271–305, 2011.

[30] L Beirao Da Veiga, Annalisa Buffa, Giancarlo Sangalli, and Rafael Vázquez. Mathematical analysis of variational isogeometric methods. *Acta Numerica*, 23:157–287, 2014.

[31] D. Doo and M. Sabin. Behaviour of recursive division surfaces near extraordinary points. *Computer-Aided Design*, 10(6):356–360, November 1978.

[32] W Dornisch, J Stöckler, and R Müller. Dual and approximate dual basis functions for b-splines and nurbs–comparison and application for an efficient coupling of patches with the isogeometric mortar method. *Computer Methods in Applied Mechanics and Engineering*, 316:449–496, 2017.

[33] W. Dornisch, J. Stöckler, and R. Müller. Dual and approximate dual basis functions for B-splines and NURBS – Comparison and application for an efficient coupling of patches with the isogeometric mortar method. *Computer Methods in Applied Mechanics and Engineering*, 316:449–496, April 2017.

[34] W. Dornisch, G. Vitucci, and S. Klinkel. The weak substitution method – an application of the mortar method for patch coupling in NURBS-

39

based isogeometric analysis. *International Journal for Numerical Methods in Engineering*, 103(3):205–234, July 2015.

[35] Wolfgang Dornisch and Sven Klinkel. Boundary conditions and multi-patch connections in isogeometric analysis. *PAMM*, 11(1):207–208, 2011.

[36] Wolfgang Dornisch and Ralf Müller. Patch coupling with the isogeometric dual mortar approach. *PAMM*, 16(1):193–194, October 2016.

[37] Michael R. Dörfel, Bert Jüttler, and Bernd Simeon. Adaptive isogeometric analysis by local h-refinement with T-splines. *Computer Methods in Applied Mechanics and Engineering*, 199(5–8):264–275, January 2010.

[38] Anand Embar, John Dolbow, and Isaac Harari. Imposing Dirichlet boundary conditions with Nitsche's method and spline-based finite elements. *International Journal for Numerical Methods in Engineering*, 83(7):877–898, August 2010.

[39] Charbel Farhat, Po-Shu Chen, and Jan Mandel. A scalable Lagrange multiplier based domain decomposition method for time-dependent problems. *International Journal for Numerical Methods in Engineering*, 38(22):3831–3853, November 1995.

[40] David R. Forsey and Richard H. Bartels. Hierarchical B-spline Refinement. In *Proceedings of the 15th Annual Conference on Computer Graphics and Interactive Techniques*, SIGGRAPH '88, pages 205–212, New York, NY, USA, 1988. ACM.

[41] Carlotta Giannelli, Bert Jüttler, and Hendrik Speleers. THB-splines: The truncated basis for hierarchical splines. *Computer Aided Geometric Design*, 29(7):485–498, October 2012.

[42] Héctor Gómez, Victor M Calo, Yuri Bazilevs, and Thomas JR Hughes. Isogeometric analysis of the cahn–hilliard phase-field model. *Computer methods in applied mechanics and engineering*, 197(49-50):4333–4352, 2008.

[43] David Groisser and Jörg Peters. Matched -constructions always yield -continuous isogeometric elements. *Computer Aided Geometric Design*, 34:67–72, March 2015.

40

[44] Yujie Guo and Martin Ruess. Nitsche's method for a coupling of isogeometric thin shells and blended shell structures. *Computer Methods in Applied Mechanics and Engineering*, 284:881–905, February 2015.

[45] Peter Hansbo. Nitsche's method for interface problems in computational mechanics. *GAMM-Mitteilungen*, 28(2):183–206, November 2005.

[46] Peter Hansbo, Carlo Lovadina, Ilaria Perugia, and Giancarlo Sangalli. A lagrange multiplier method for the finite element solution of elliptic interface problems using non-matching meshes. *Numerische Mathematik*, 100(1):91–115, 2005.

[47] Christian Hesch and Peter Betsch. Isogeometric analysis and domain decomposition methods. *Computer Methods in Applied Mechanics and Engineering*, 213–216:104–112, March 2012.

[48] Stefan Hüeber and Barbara I Wohlmuth. A primal–dual active set strategy for non-linear multibody contact problems. *Computer Methods in Applied Mechanics and Engineering*, 194(27-29):3147–3166, 2005.

[49] T.J.R. Hughes, J.A. Cottrell, and Y. Bazilevs. Isogeometric analysis: Cad, finite elements, nurbs, exact geometry and mesh refinement. *Computer Methods in Applied Mechanics and Engineering*, 194(39):4135 – 4195, 2005.

[50] Mika Juntunen. On the connection between the stabilized lagrange multiplier and nitsche's methods. *Numerische Mathematik*, 131(3):453–471, 2015.

[51] Bert Jüttler, Angelos Mantzaflaris, Ricardo Perl, and Martin Rumpf. On numerical integration in isogeometric subdivision methods for PDEs on surfaces. *Computer Methods in Applied Mechanics and Engineering*, 302:131–146, April 2016.

[52] Hongmei Kang, Xin Li, Falai Chen, and Jiansong Deng. Truncated Hierarchical Loop Subdivision Surfaces and application in isogeometric analysis. *Computers & Mathematics with Applications*, 72(8):2041–2055, October 2016.

[53] Mario Kapl, Florian Buchegger, Michel Bercovier, and Bert Jüttler. Isogeometric analysis with geometrically continuous functions on planar

896 multi-patch geometries. *Computer Methods in Applied Mechanics and*
897 *Engineering*, 316:209–234, April 2017.

898 [54] Mario Kapl and Vito Vitrih. Space of -smooth geometrically continuous
899 isogeometric functions on planar multi-patch geometries: Dimension and
900 numerical experiments. *Computers & Mathematics with Applications*.

901 [55] Mario Kapl and Vito Vitrih. Space of -smooth geometrically continuous
902 isogeometric functions on two-patch geometries. *Computers & Mathe-*
903 *matics with Applications*, 73(1):37–59, January 2017.

904 [56] Mario Kapl, Vito Vitrih, Bert Jüttler, and Katharina Birner. Isoge-
905 ometric analysis with geometrically continuous functions on two-patch
906 geometries. *Computers & Mathematics with Applications*, 70(7):1518–
907 1538, October 2015.

908 [57] J Kiendl, Y Bazilevs, M-C Hsu, R Wüchner, and K-U Bletzinger. The
909 bending strip method for isogeometric analysis of kirchhoff–love shell
910 structures comprised of multiple patches. *Computer Methods in Applied*
911 *Mechanics and Engineering*, 199(37-40):2403–2416, 2010.

912 [58] J Kiendl, K-U Bletzinger, J Linhard, and R Wüchner. Isogeometric shell
913 analysis with kirchhoff–love elements. *Computer Methods in Applied*
914 *Mechanics and Engineering*, 198(49-52):3902–3914, 2009.

915 [59] Josef Kiendl, Ming-Chen Hsu, Michael CH Wu, and Alessandro Reali.
916 Isogeometric kirchhoff–love shell formulations for general hyperelastic
917 materials. *Computer Methods in Applied Mechanics and Engineering*,
918 291:280–303, 2015.

919 [60] Bishnu Prasad Lamichhane. Higher order mortar finite elements with
920 dual lagrange multiplier spaces and applications.

921 [61] Bishnu Prasad Lamichhane and Barbara I Wohlmuth. Higher order
922 dual lagrange multiplier spaces for mortar finite element discretizations.
923 *Calcolo*, 39(4):219–237, 2002.

924 [62] Xin Li and M. A. Scott. Analysis-suitable T-splines: Characterization,
925 refineability, and approximation. *Mathematical Models and Methods in*
926 *Applied Sciences*, 24(06):1141–1164, October 2013.

[63] Xin Li, Jianmin Zheng, Thomas W. Sederberg, Thomas J. R. Hughes, and Michael A. Scott. On linear independence of T-spline blending functions. *Computer Aided Geometric Design*, 29(1):63–76, January 2012.

[64] Charles Teorell Loop and Charles Loop. Smooth Subdivision Surfaces Based on Triangles. January 1987.

[65] Leszek Marcinkowski. Mortar methods for some second and fourth order elliptic equations. *Distinguished Ph. D. Thesis*, 1999.

[66] Stephen E Moore. Discontinuous galerkin isogeometric analysis for the biharmonic equation. *arXiv preprint arXiv:1703.02726*, 2017.

[67] Thien Nguyen, Keçstutis Karčiauskas, and Jörg Peters. A Comparative Study of Several Classical, Discrete Differential and Isogeometric Methods for Solving Poisson's Equation on the Disk. *Axioms*, 3(2):280–299, June 2014.

[68] Vinh Phu Nguyen, Pierre Kerfriden, Marco Brino, Stéphane P. A. Bordas, and Elvio Bonisoli. Nitsche's method for two and three dimensional NURBS patch coupling. *Computational Mechanics*, 53(6):1163–1182, June 2014.

[69] J. Nitsche. Über ein Variationsprinzip zur Lösung von Dirichlet-Problemen bei Verwendung von Teilräumen, die keinen Randbedingungen unterworfen sind. *Abhandlungen aus dem Mathematischen Seminar der Universität Hamburg*, 36(1):9–15, July 1971.

[70] Qing Pan, Guoliang Xu, Gang Xu, and Yongjie Zhang. Isogeometric analysis based on extended Loop's subdivision. *Journal of Computational Physics*, 299:731–746, October 2015.

[71] Jörg Peters. Joining smooth patches around a vertex to form a Ck surface. *Computer Aided Geometric Design*, 9(5):387–411, November 1992.

[72] Jörg Peters. Chapter 8 - Geometric Continuity. In *Handbook of Computer Aided Geometric Design*, pages 193–227. North-Holland, Amsterdam, 2002. DOI: 10.1016/B978-044451104-1/50009-5.

[73] Alexander Popp, Michael W Gee, and Wolfgang A Wall. A finite deformation mortar contact formulation using a primal–dual active set strategy. *International Journal for Numerical Methods in Engineering*, 79(11):1354–1391, 2009.

[74] Beatrice Riviere. *Discontinuous Galerkin methods for solving elliptic and parabolic equations: theory and implementation*. SIAM, 2008.

[75] M. A. Scott, X. Li, T. W. Sederberg, and T. J. R. Hughes. Local refinement of analysis-suitable T-splines. *Computer Methods in Applied Mechanics and Engineering*, 213–216:206–222, March 2012.

[76] M. A. Scott, R. N. Simpson, J. A. Evans, S. Lipton, S. P. A. Bordas, T. J. R. Hughes, and T. W. Sederberg. Isogeometric boundary element analysis using unstructured T-splines. *Computer Methods in Applied Mechanics and Engineering*, 254:197–221, February 2013.

[77] Michael A. Scott, Michael J. Borden, Clemens V. Verhoosel, Thomas W. Sederberg, and Thomas J. R. Hughes. Isogeometric finite element data structures based on Bézier extraction of T-splines. *International Journal for Numerical Methods in Engineering*, 88(2):126–156, October 2011.

[78] Thomas W. Sederberg, Jianmin Zheng, Almaz Bakenov, and Ahmad Nasri. T-splines and T-NURCCs. In *ACM SIGGRAPH 2003 Papers*, SIGGRAPH '03, pages 477–484, New York, NY, USA, 2003. ACM.

[79] Alexander Seitz, Philipp Farah, Johannes Kremheller, Barbara I. Wohlmuth, Wolfgang A. Wall, and Alexander Popp. Isogeometric dual mortar methods for computational contact mechanics. *Computer Methods in Applied Mechanics and Engineering*, 301:259–280, April 2016.

[80] Juan C Simo, Peter Wriggers, and Robert L Taylor. A perturbed lagrangian formulation for the finite element solution of contact problems. *Computer methods in applied mechanics and engineering*, 50(2):163–180, 1985.

[81] Rolf Stenberg. On some techniques for approximating boundary conditions in the finite element method. *Journal of Computational and applied Mathematics*, 63(1-3):139–148, 1995.

44

[82] Gilbert Strang and George Fix. *An Analysis of the Finite Element Method.* Wellesley-Cambridge Press, May 2008. Google-Books-ID: K5MAOwAACAAJ.

[83] Radek Tezaur. *Analysis of Lagrange multiplier based domain decomposition.* PhD thesis, University of Colorado at Denver, 1998.

[84] Derek C Thomas, Michael A Scott, John A Evans, Kevin Tew, and Emily J Evans. Bézier projection: a unified approach for local projection and quadrature-free refinement and coarsening of nurbs and t-splines with particular application to isogeometric design and analysis. *Computer Methods in Applied Mechanics and Engineering*, 284:55–105, 2015.

[85] Manuel Tur, Jose Albelda, Jose Manuel Navarro-Jimenez, and Juan Jose Rodenas. A modified perturbed lagrangian formulation for contact problems. *Computational Mechanics*, 55(4):737–754, 2015.

[86] A. V. Vuong, C. Giannelli, B. Jüttler, and B. Simeon. A hierarchical approach to adaptive local refinement in isogeometric analysis. *Computer Methods in Applied Mechanics and Engineering*, 200(49–52):3554–3567, December 2011.

[87] Xiaodong Wei, Yongjie Zhang, Thomas J. R. Hughes, and Michael A. Scott. Truncated hierarchical Catmull–Clark subdivision with local refinement. *Computer Methods in Applied Mechanics and Engineering*, 291:1–20, July 2015.

[88] B. Wohlmuth. A Mortar Finite Element Method Using Dual Spaces for the Lagrange Multiplier. *SIAM Journal on Numerical Analysis*, 38(3):989–1012, January 2000.

[89] Barbara I Wohlmuth. A comparison of dual lagrange multiplier spaces for mortar finite element discretizations. *ESAIM: Mathematical Modelling and Numerical Analysis*, 36(6):995–1012, 2002.

[90] Xin Li. Some Properties for Analysis-Suitable T-Splines. *Journal of Computational Mathematics*, 33(4):428–442, July 2015.

[91] Olgierd Cecil Zienkiewicz, Robert Leroy Taylor, Olgierd Cecil Zienkiewicz, and Robert Lee Taylor. *The finite element method*, volume 3. McGraw-hill London, 1977.